Operational tolerance after hematopoietic stem cell transplantation is characterized by distinct transcriptional, phenotypic, and metabolic signatures

Dubouchet, Laetitia; Todorov, Helena; Seurinck, Ruth; Vallet, Nicolas; Van Gassen, Sofie; Corneau, Aurélien; Blanc, Catherine; Zouali, Habib; Boland, Anne; Deleuze, Jean-François; Ingram, Brian; de Latour, Regis Peffault; Saeys, Yvan; Socié, Gérard [**and 1 more**]

TRANSPLANTATION

Operational tolerance after hematopoietic stem cell transplantation is characterized by distinct transcriptional, phenotypic, and metabolic signatures

Laetitia Dubouchet[1]†, Helena Todorov[2,3]†, Ruth Seurinck[2,3], Nicolas Vallet[1], Sofie Van Gassen[2,3], Aurélien Corneau[4], Catherine Blanc[4], Habib Zouali[5], Anne Boland[6], Jean-François Deleuze[5,6], Brian Ingram[7], Regis Peffault de Latour[8], Yvan Saeys[2,3], Gérard Socié[1,8]*‡, David Michonneau[1,8]*‡

The mechanisms underlying operational tolerance after hematopoietic stem cell transplantation in humans are poorly understood. We studied two independent cohorts of patients who underwent allogeneic hematopoietic stem cell transplantation from human leukocyte antigen–identical siblings. Primary tolerance was associated with long-lasting reshaping of the recipients' immune system compared to their healthy donors with an increased proportion of regulatory T cell subsets and decreased T cell activation, proliferation, and migration. Transcriptomics profiles also identified a role for nicotinamide adenine dinucleotide biosynthesis in the regulation of immune cell functions. We then compared individuals with operational tolerance and nontolerant recipients at the phenotypic, transcriptomic, and metabolomic level. We observed alterations centered on CD38$^+$-activated T and B cells in nontolerant patients. In tolerant patients, cell subsets with regulatory functions were prominent. RNA sequencing analyses highlighted modifications in the tolerant patients' transcriptomic profiles, particularly with overexpression of the ectoenzyme *NT5E* (encoding CD73), which could counterbalance CD38 enzymatic functions by producing adenosine. Further, metabolomic analyses suggested a central role of androgens in establishing operational tolerance. These data were confirmed using an integrative approach to evaluating the immune landscape associated with operational tolerance. Thus, balance between a CD38-activated immune state and CD73-related production of adenosine may be a key regulator of operational tolerance.

INTRODUCTION

The concept of tolerance was first introduced in 1953 by Billingham *et al.* (*1*) who demonstrated that exposure to a foreign antigen during fetal life could induce immune tolerance. Immune tolerance is classically divided into central and peripheral tolerance. Central tolerance includes negative selection of autoreactive lymphocytes and expansion of natural regulatory T cells in the thymus (*2*). The breakdown, or the defect, of central tolerance can lead to autoimmunity (*3*). Peripheral tolerance is due to self-reactive T cells unresponsiveness or deletion after encountering peripheral self-antigens. Peripheral tolerance plays a major role in pregnancy, in autoimmunity (*4*), and in graft rejection after solid organ transplantation (*5*).

In the setting of solid organ transplantation, rare patients have a functional graft and no sign of rejection, although all immunosuppressive (IS) drugs have been withdrawn. This lack of alloreactivity has been named operational tolerance (*6*–*9*). Immune mechanisms underlying the induction and the maintenance of operational tolerance have been studied after solid organ transplantation, with a particular focus on the role of regulatory CD4$^+$ T cells, natural killer (NK) cells (*10*), regulatory B cells (*11*–*16*), and mixed hematopoietic chimerism (*17*). Transient mixed chimerism–based tolerance induction could be peripheral, relying on both expansion of regulatory T cells and deletion of donor-specific effector T cells (*18*), and central with thymic colonization by donor-derived dendritic cells and negative selection of donor-reactive T cells (*19*, *20*). Last, it has been proposed that immune tolerance might not only be due to the absence of immune response against foreign antigen but could also be due to intrinsic tissue tolerance (*21*, *22*).

Despite some similarities with solid organ transplantation, allogeneic hematopoietic stem cell transplantation (allo-HSCT) differs from an immunological point of view. During allo-HSCT, the whole donor's immune system must face antigen incompatibilities in the recipient. Furthermore, in patients with hematologic malignancy, the donor's immune system prevents relapse through a graft-versus-tumor (GvT) effect (*23*–*25*). However, allo-HSCT is also hampered by frequent occurrence of acute or chronic graft-versus-host disease (GvHD) (*26*, *27*). Although operational tolerance is the exception after solid organ transplantation, it occurs far more frequently after allo-HSCT, with long-lasting absence of GvHD despite IS drugs withdrawal. Complete donor hematopoietic chimerism with operational tolerance can thus be considered as the result of combined effective GvT, without GvHD, a recent emerging composite end point named GvHD-free/relapse-free survival (*28*). Understanding the biological mechanisms of operational tolerance in this setting is thus of major biological and clinical interest.

Here, we conducted a study to characterize tolerance mechanisms in patients grafted from a human leukocyte antigen (HLA)–identical sibling donor. In this HLA-matched setting, tolerant recipients

[1]Université de Paris, INSERM U976, F-75010 Paris, France. [2]Data Mining and Modeling for Biomedicine, VIB Center for Inflammation Research, 9052 Ghent, Belgium. [3]Department of Applied Mathematics, Computer Science and Statistics, Ghent University, 9052 Ghent, Belgium. [4]Plateforme de Cytométrie de la Pitié-Salpétrière (CyPS), UMS037–PASS, Sorbonne Université–Faculté de Médecine, F-75013 Paris, France. [5]Centre d'étude du polymorphisme humain, 75010 Paris, France. [6]Université Paris-Saclay, CEA, Centre National de Recherche en Génomique Humaine, 91057 Evry, France. [7]Metabolon Inc., Morrisville, NC 27560, USA. [8]Hematology Transplantation, Saint Louis Hospital, 1 Avenue Claude Vellefaux, 75010 Paris, France.
*Corresponding author. Email: david.michonneau@aphp.fr (D.M.); gerard.socie@aphp.fr (G.S.)
†These authors contributed equally to this work.
‡These authors contributed equally to this work.

have a fully functional immune system, able to prevent hematologic relapse, to control infections and do not present symptoms of immune deficiency. We hypothesized that operational tolerance emerges from a global immune system adaptation after allo-HSCT. The aim of this study was to decipher the immune landscape associated with operational tolerance using deep cell immunophenotyping, transcriptomics, and metabolomic profiles. Using a combination of statistical analyses and systems immunology methods, we identified biological parameters characterizing tolerance.

RESULTS

Immune profiling after allo-HSCT using multiomics

To determine how the donor's immune system is reshaped by allo-HSCT and what biological changes are associated with operational tolerance, we collected blood samples from recipients who underwent an HLA-matched allo-HSCT from a sibling donor (thus avoiding an HLA mismatch situation). Peripheral blood mononuclear cells (PBMCs) and plasma obtained 1 to 2 years after transplantation in recipients, or before HSC collection in donors, were cryopreserved. Healthy sibling donors were considered as paired controls because they represent the same immune system at baseline. We used mass cytometry, RNA sequencing, and metabolomics profiling with ultrahigh-performance liquid chromatography in tandem with mass spectrometry (UPLC-MS/MS) (Fig. 1A). Two cohorts of patients were explored (Fig. 1B): a monocentric cohort of 41 patients and a second multicentric cohort of 69 patients. All patients had a full donor chimerism at the time of sampling. For each patient-donor pair, biological data (immunophenotypic, transcriptomics, and metabolomics profile) and clinical data were collected and analyzed. The patients were classified into three stages of tolerance: (i) Patients who did not develop acute or chronic GvHD and whose IS drugs had been withdrawn since several months at the time of sample (median delay between IS stop and sampling, 8.4 months; range, 2 to 21 months) were classified as primary operational tolerant and did not develop GvHD after sampling (median follow-up, 45 months; range, 1 to 74 months). (ii) Patients who experienced acute or chronic GvHD but to whom IS were lastly stopped (median delay between IS stop and sampling, 7 months; range, 1 to 27 months before sampling) without GvHD flare until last follow-up (median follow-up, after 31 months; range, 1 to 70 months) were referred to as secondary tolerant. (iii) Last, patients who developed acute or chronic GvHD and to whom physicians were unable to stop IS drugs were considered as nontolerant (median follow-up, 30 months after sampling; range, 2 to 80 months) (table S1).

Data mining integrates multiomics and clinical data to unravel immune variation associated with tolerance

The phenotypic, transcriptomic, and metabolomic data were preprocessed as described in Materials and Methods. For mass cytometry phenotypic data, clustering was performed using the FlowSOM algorithm in an unsupervised approach (*29*). Forty metaclusters were defined, and their immune phenotypes were manually verified to identify their corresponding immune cell subsets (fig. S1). A supervised feature selection approach was then performed to identify biological variables that were associated with tolerance. The association between each variable and tolerance was derived through logistic regression models. The resulting area under the curve (AUC) was compared to a permutation distribution that resulted from 1000 logistic regression models applied on permuted tolerance values for each variable. Biological variables for which the observed AUC exceeded 90% of all permuted AUCs [quantile AUC (qAUC) > 0.9] were selected. We applied a two-step comparison of tolerant versus nontolerant patients and of primary versus secondary tolerant patients. All analyses were performed separately in both cohorts. For each modality, we compared the biological variables identified in the monocentric and the multicentric cohorts, and we retained those that were identified in both cohorts with a qAUC of >0.9 in the permutation distributions. These selected biological variables were then used to build a final integrative analysis to identify correlations among phenotypic, transcriptomic, and metabolomic variables (Fig. 1C). The association of clinical characteristics with the patient's tolerance status was analyzed in both cohorts (Fig. 1D and table S1). Furthermore, we performed a multinomial logistic regression analysis to identify relevant clinical factors that influence the probability of tolerance (fig. S2). We observed that the odds ratio of nontolerance relative to primary tolerance increased with recipients' age, peripheral blood stem cell graft source, the absence of antithymocyte globulin (ATG) and a donor's seropositive cytomegalovirus (CMV) status. Previous studies had already identified age (*30*), graft source (*31*, *32*), use of ATG (*33*), and CMV status (*34*) as risk factors for acute or chronic GvHD. No association was found between tolerance and gender matching or blood group compatibility. Last, we performed integrative analyses including the biological variables that were significantly ($P < 0.05$) associated with tolerance in both cohorts and had the same behavior in patients from both cohorts. At the final stage, for each selected biological variable included in the integrative analysis, the relative contribution of age and gender was assessed by additional post hoc logistic regression models. We also evaluated the association of the resulting integrated components with recipients' age, graft source, ATG, and CMV status in donors as potential major clinical confounders.

Donor immune profiles only partially explain posttransplantation tolerance status

We first analyzed differences between donors from tolerant or nontolerant recipients to determine whether preexisting variations in the donor's immune system could influence the outcome (fig. S3A) (*35*). We compared the abundance of immune subsets using feature selection methods and identified two immune subsets that discriminated donors from tolerant recipients and donors from nontolerant recipients. We also identified three immune subsets that differentiated donors from primary tolerant recipients and donors from secondary tolerant recipients (fig. S3, B and C). However, only one cell subset, namely, $CD38^{+}FoxP3^{+}$ cells, was consistently retrieved in both cohorts for the comparison of donors from tolerant and nontolerant recipients (fig. S3D). A similar approach was used to identify genes that were differentially expressed in donors according to the recipients' outcome (fig. S3, E and F), but no gene expression was significantly associated with outcome in both cohorts after *t* test with correction for multiple comparisons ($P > 0.05$). Last, the comparison of the donors' metabolome identified few metabolites associated with the recipient's outcome, with androstenediol (3β,17β) disulfate being significantly increased in both cohorts in donors of tolerant recipients (cohort 1, $P = 0.008$; cohort 2, $P = 0.03$) (fig. S3, G and H). Together, these results suggest that the tolerance status after transplantation is only marginally explained by immunological, transcriptomics, or metabolomics characteristics of the donors.

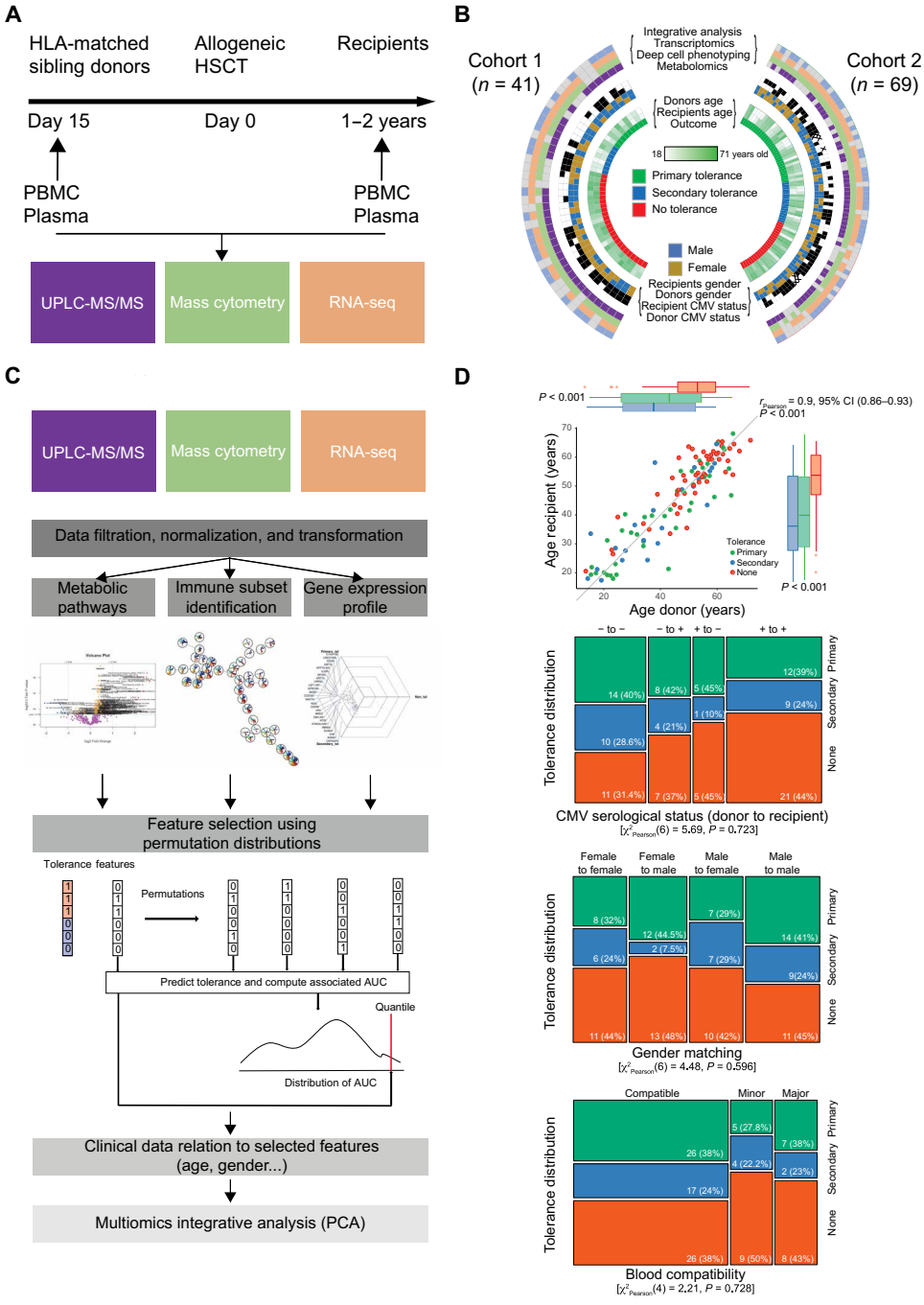

Fig. 1. Study overview of biological and clinical data analysis. (**A**) Recipients who underwent allo-HSCT were sampled 1 to 2 years after transplantation, and their related sibling donors, used as healthy controls, were sampled before stem cell collection. RNA-seq, RNA sequencing. (**B**) Forty-one patients from a monocentric cohort (cohort 1, Saint Louis hospital) and 73 patients from a multicentric national cohort (cohort 2, CRYOSTEM Consortium) were analyzed separately. Clinical data, metabolomics (purple), mass cytometry (light green), and transcriptomics profile (orange) were analyzed for donors and recipients. Each patient was classified as primary tolerant (green), secondary tolerant (blue), or as not tolerant (red). (**C**) Data analysis consisted of multiple steps including data cleaning, feature selection and quantification for all three biological approaches. Biological variables associated with the clinical outcome were selected using logistic regression models. For each parameter a permutation distribution was generated for the area under the curve (AUC) of the corresponding receiver operating characteristic (ROC) curve. Only if the observed AUC exceeded 90% of all permuted AUCs (qAUC > 0.9) in both cohorts was the feature was considered informative for the outcome. To control for additional clinical characteristics, logistic regression models were performed with selected biological variables and relevant clinical variables to estimate the influence of clinical parameters on the association between biological data and tolerance and used for a final integrative analysis. (**D**) Clinical variables associated with tolerance were identified using a Kruskal-Wallis test for continuous variables or a chi-squared test for categorical variables, and *P* values were adjusted using a Benjamini-Hochberg correction for multiple testing. Results are presented for some relevant clinical variables associated with outcome (age) or that may have a significant impact on biological variable [CMV serological status, gender, and blood (ABO) compatibility]. See also table S1 for whole clinical variables analysis. CI, confidence interval.

Primary tolerant recipients have increased abundance of regulatory subsets and decreased T cell activation compared to their donors

Because the mechanisms that reshape the immune system during tolerance after allo-HSCT are currently unknown, we compared each group of recipients with their related donors. First, paired primary tolerant recipient and donor samples were compared in both cohorts (cohort 1, $n = 9$; cohort 2, $n = 32$). Nine FlowSOM metaclusters were identified (Fig. 2A and fig. S4). Primary tolerant recipients exhibited a higher frequency of naïve B cells (metacluster 25), $CD4^+CD25^+FoxP3^-$ T cells (metacluster 26), and an increased frequency of $CD4^+FoxP3^+OX40^+$ regulatory T cells (metacluster 30). Primary tolerance was also associated with an increased frequency of $CD25^+$ double-positive T cells (metacluster 8), previously described as an interferon-γ (IFN-γ)–dependent suppressive population (*36*–*38*). Simultaneously, $CD8^+$ inducible T cell costimulator–positive ($ICOS^+$) central memory T cells (metacluster 10), $CD8^+FoxP3^+$ T cells, and $CD25^+$ B cells were decreased (Fig. 2A and fig. S4). No cell subset differed between secondary tolerant recipients and their donors. Four hundred sixty-four genes were differentially expressed between donors and primary tolerant recipients (data file S1). A pathway analysis revealed an enrichment of process associated with immune cell function, especially cell-to-cell signaling and interaction, cellular growth, proliferation, and immune cell migration (Fig. 2B). Analysis of metabolic and signaling pathways highlighted enrichment of many pathways involved in cell cycle regulation and decreased expression of genes involved in metabolism or in cell signaling [neuronal nitric oxide synthase (nNOS), adenosine 3′,5′-monophosphate (cAMP), and protein kinase A signaling] (Fig. 2C). Again, no differentially expressed gene was identified by comparison of secondary tolerant recipients with their donors. Together, these results reveal that primary tolerance is associated with long-lasting reshaping of the immune system of primary tolerant recipients compared to their healthy donors and suggest that primary tolerance is associated with an increased proportion of regulatory T cell subsets and a decrease in T cell activation, proliferation, and migration.

Nontolerant recipients exhibit a persistent immune activation state relative to their donors

We then compared nontolerant recipients with their paired donors. We first identified 30 immune subsets that were significantly ($P < 0.05$) different in both cohorts (Fig. 2D and fig. S5). Nontolerant recipients were characterized by decreased abundance of naïve $CD4^+$, $CD8^+$ and double-negative (DN) T cells, naïve and memory B cells, and cytotoxic T lymphocyte–associated protein 4 (CTLA4)–expressing effector memory $CD4^+$ T cells. At the same time, many immune subsets were increased in nontolerant recipients relative to their donors, most of them expressing activation marker such as CD25, granzyme B, and CD38. We then compared gene expression between nontolerant recipients and their donors and identified 1159 genes that were differentially expressed in both cohorts (data file S2). Pathways associated with these genes corresponding to main biological process (Fig. 2E) or signaling pathways (Fig. 2F and data file S3) reveal that absence of tolerance was associated with genes involved in expansion, activation, and migration of T and B cells. This was associated with metabolic and signaling pathways including complement activation, planar cell polarity (PCP) and Wnt signaling, fibrosis, and pyrimidine biosynthesis. The *CD38* gene was overexpressed in nontolerant recipients (cohort 1, $P = 0.002$; cohort 2, $P = 0.001$), consistent with the mass cytometry results. Together, these results support the hypothesis of a long-lasting immune activation involving both T and B cells.

Thus, comparing the immune system at baseline in healthy donors to their respective recipients revealed an active regulatory network associated with primary tolerance, whereas the lack of tolerance was characterized by a state of hyperimmune reaction. With the aim of dissecting these results in depth, we then compared the three immune states at the phenotypic, transcriptomic, and metabolomic level between recipients before proceeding to integrative analyses.

Immunophenotyping identifies DN regulatory, $CD8^+$ naïve, and central memory T cells in tolerant recipients, whereas nontolerant patients exhibit increased CD38 expression on immune cells

Immune profiles of recipients from both cohorts were then compared according to their outcome (Fig. 3A). Two sets of comparisons were performed: first, tolerant recipients versus nontolerant recipients and then primary versus secondary tolerant recipients (Fig. 3B). In tolerant recipients, three metaclusters were overrepresented, $CD8^+$ naïve T cells (metacluster 4), $CCR5^+CD8^+$ central memory T cells (metacluster 7), and DN T cells (metacluster 23). DN T cells have been described as a rare regulatory subset (*39*–*41*). They have been characterized by their in vitro suppressive properties under allogeneic conditions (*42*) and could inhibit the allogeneic response (*43*).

By contrast, nontolerant recipients were characterized by an increased proportion of 21 metaclusters, which were grouped in correlation maps within three clusters of cells characterized by the expression of CD38, CTLA4, or CD24 (Fig. 3C and fig. S6). Analyses performed on pooled data from both cohorts are also shown in Fig. 3D. CD38 overexpression was observed on central and effector memory T cells, DN T cells, NK cells, and naïve B cells, similarly to what we observed in comparing donors and nontolerant recipients (Fig. 2B), further suggesting a central role for CD38 in sustained immune responses in nontolerant patients. Last, the comparison of primary and secondary tolerant patients revealed a significant increase in $CD38^+$ $CD4^+$ regulatory T cells (metacluster 29) in secondary tolerant patients in both cohorts (cohort 1, $P = 0.02$; cohort 2, $P = 0.03$) (Fig. 3E). In summary, mass cytometry data suggested that many phenotypic alterations mainly centered on $CD38^+$-activated T and B cells in nontolerant patients, whereas in tolerant patients, cell subsets with regulatory functions emerged.

Transcriptional changes associated with tolerance highlight a role for *NT5E* nucleotidase activity, T cell stemness, and cell cycle regulation

Gene expression profiles of patients in each of the three groups were compared together using Triwise plots (*44*) to identify genes that were differentially expressed between primary tolerant, secondary tolerant, and nontolerant recipients. Two hundred twenty-seven genes (data file S4) and 118 genes (data file S5) were overexpressed in primary and secondary tolerant recipients, respectively, compared to nontolerant ones (Fig. 4A). Among genes involved in the regulation of the immune response, we observed increased expression of not only genes associated with stemness properties of T cells, such as *LEF1* and *TCF7* (*45*–*47*), but also in genes involved in the regulation of immune response, migration, and differentiation (Fig. 4B). In addition, genes involved in Wnt (*WNT7A*) and guanosine triphosphatase (GTPase) signaling (*RASGRF2* and *DEPDC7*) were

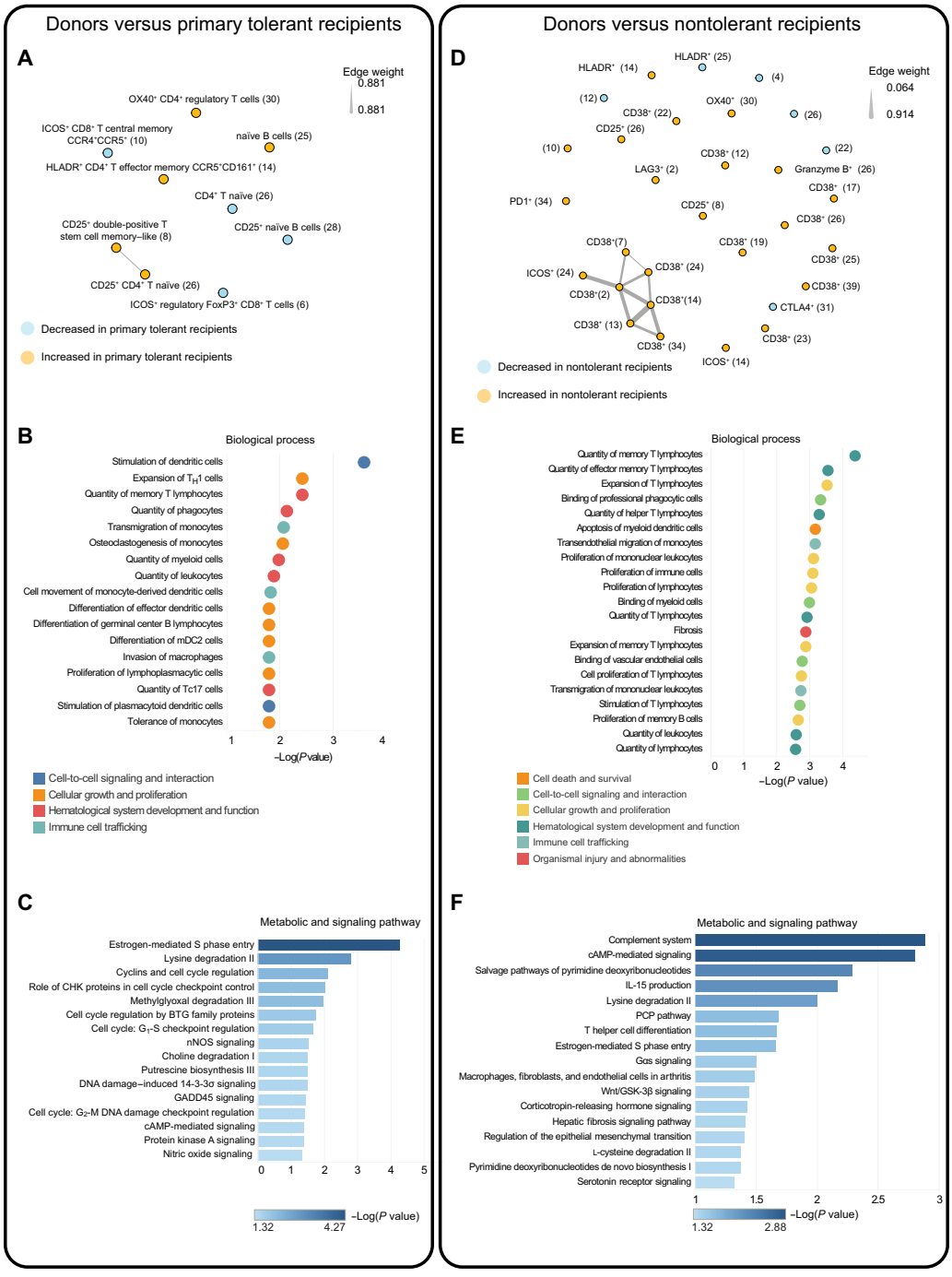

Fig. 2. Immune phenotyping and transcriptomics profile of patients compared to their donors. For each group of patients (primary tolerant, secondary tolerant, or nontolerant), recipients were compared to their related donors in both cohorts. (**A**) Compared to donors, five metaclusters were overrepresented in primary tolerant patients (orange) and four were decreased (blue). (**B**) Four hundred sixty-four genes were differentially expressed between donors and primary tolerant recipients (full list available in data file S1). The graph illustrates the overrepresentation analysis of biological processes associated with primary tolerance (Fisher's exact test with $P < 0.05$). Dots are colored by generic biological function. (**C**) Graph showing the overrepresentation analysis of signaling and metabolic pathways associated with primary tolerance (Fisher's exact test with $P < 0.05$) (**D**) Comparison of nontolerant recipients with their donors identified 30 metaclusters being increased (orange) or decreased (blue) in recipients. Correlation maps represent correlations between metaclusters (nodes identified by metaclusters' number and functional markers) that were retrieved in both cohorts with $P < 0.001$ (gray edges). Line width is proportional to the R correlation coefficient (edge weight). (**E**) One thousand nine hundred fifty-nine genes were differentially expressed between nontolerant recipients and their donors in both cohorts (full list available in data file S2). The graph illustrates the overrepresentation analysis of the main biological processes. Dots are colored by generic biological function. (**F**) Graph showing the overrepresentation analysis of signaling and metabolic pathways associated with the absence of tolerance (Fisher's exact test with $P < 0.05$) (full list of pathways available in data file S3). All P values were adjusted using Benjamini-Hochberg correction for multiple testing.

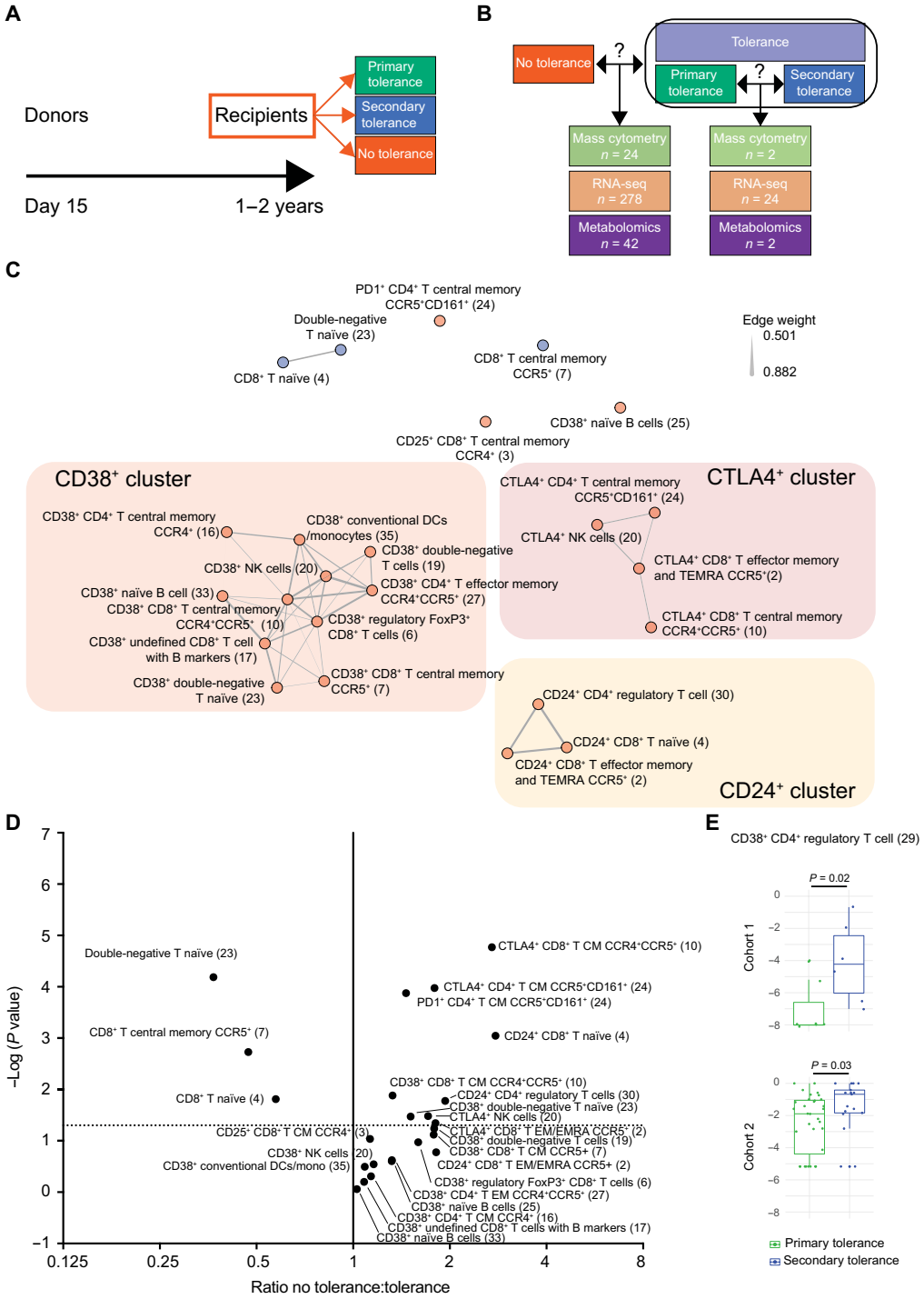

Fig. 3. Comparison of recipients according to the outcome and immunophenotyping results. (**A**) Phenotypic, transcriptomic, and metabolomics data from recipients were compared according to their clinical outcome. (**B**) Comparison of tolerant recipients with nontolerant recipients with logistic regression models and feature permutations led to the identification of 24 metaclusters, 278 genes, and 42 metabolites in both cohorts (based on AUC > 0.9). A second comparison of primary tolerant and secondary tolerant recipients identified two metaclusters, 24 genes, and two metabolites that distinguished both groups. (**C**) A correlation map was built with the 24 metaclusters that differed between tolerant and nontolerant recipients to identify cell subsets (nodes) that were correlated in both cohorts. Edge thickness represents the mean correlation coefficient (Spearman correlation test, $P < 0.001$). Three metaclusters were increased in tolerant recipients (blue), and 21 were increased in nontolerant patients (red). Three clusters of highly correlated populations were identified in nontolerant patients, associated with expression of CD38, CD24, or CTLA4. DC, dendritic cell. TEMRA, effector memory T cells re-expresses CD45RA. (**D**) A volcano plot representing fold change (FC) analysis and *P* value is shown for recipients pooled from both cohorts (cohort 1, $n = 34$; cohort 2, $n = 69$). See also fig. S6 for individual representations of the 24 immune subsets frequencies. (**E**) Comparison of primary and secondary tolerant recipients identified $CD38^+$ $CD4^+$ regulatory T cells as the only significant subsets in both cohorts. All *P* values are adjusted after Benjamini-Hochberg correction for multiple testing.

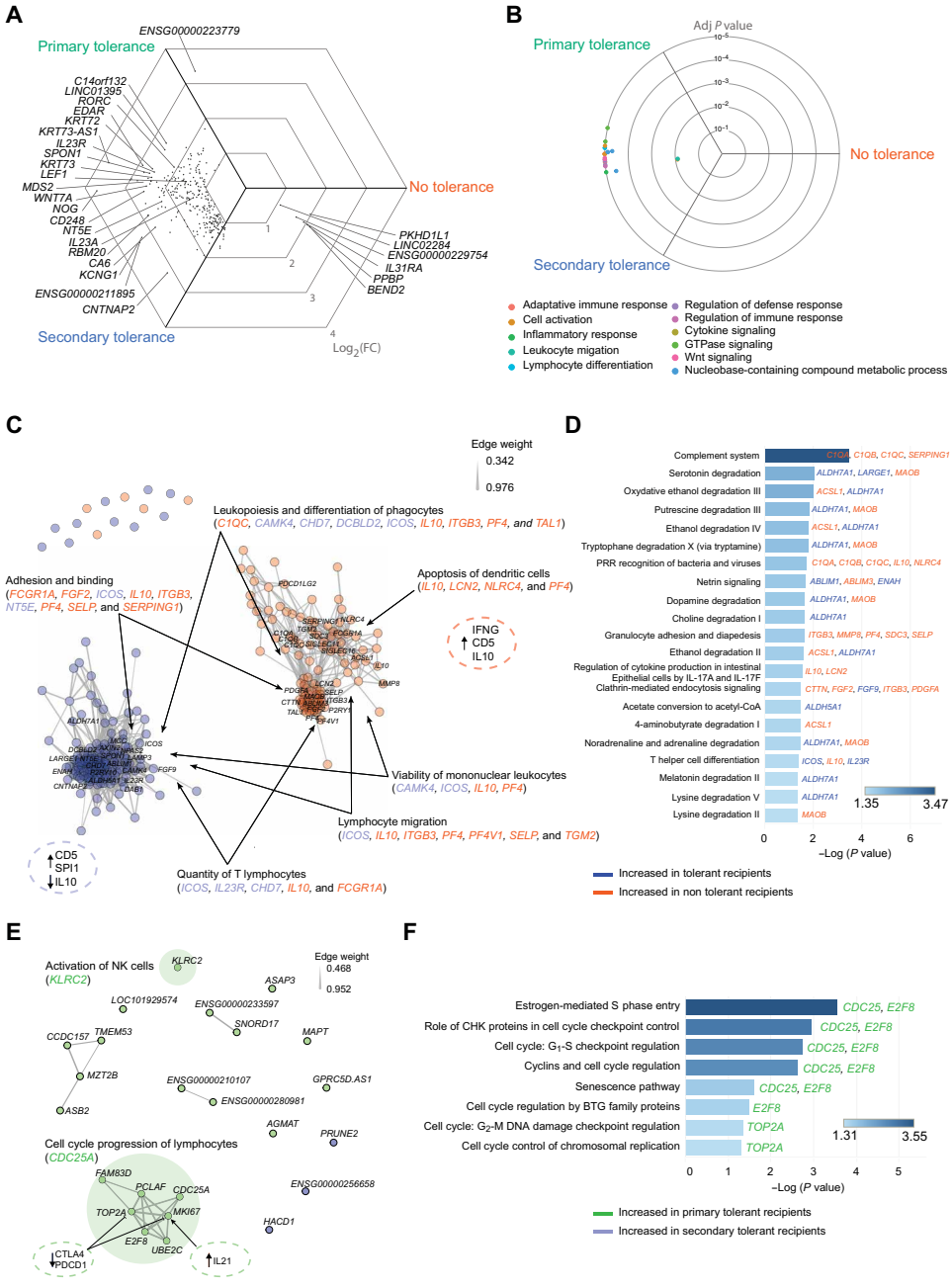

Fig. 4. Transcriptomics profiling distinguishes recipients in tolerant and nontolerant recipients. (**A**) Recipients' transcriptomics profiles were first compared between the three groups (primary tolerant, secondary tolerant, and nontolerant recipients) to identify differentially expressed genes. Results are represented using a Triwise plot. Two hundred twenty-seven genes were differentially expressed between primary tolerant and nontolerant patients (data file S4), and 118 genes were differentially expressed between secondary tolerant and nontolerant patients (FC > 2 and adjusted $P < 0.05$ with Benjamini-Hochberg correction) (data file S5). (**B**) Enrichment analysis was completed using Gene Ontology:Biological Process (GO:BP) (Fisher's exact test, $P < 0.0001$ and lowest redundancy). GO pathways were grouped in modules, and statistical significance is presented in the direction of the circular mean for differentially expressed genes. (**C**) A correlation map was built to identify correlations between the genes that differed significantly between tolerant and nontolerant recipients ($n = 278$) (data file S6). Genes with AUC > 0.9 in both cohorts were represented as blue nodes when increased in tolerant recipients and red nodes when increased in nontolerant recipients. Nodes are connected with edges when gene expression was correlated together in both cohorts (Spearman correlation test, $P < 0.001$). Enrichment of biological processes were analyzed with ingenuity pathway analysis (IPA) and grouped in main modules, with gene names in blue when increased in tolerant recipients and red when increased in nontolerant recipients (Fisher's exact test, $P < 0.01$). Upstream regulators were predicted with IPA and represented inside the dashed line circle ($P < 0.01$). (**D**) Enrichment of metabolic and signaling pathways were calculated with IPA and ranked by −log(*P* value). (**E**) Logistic regression models and feature permutations were used to identify genes that distinguished primary and secondary tolerant patients ($n = 24$). Genes with AUC > 0.9 in both cohorts were represented as green nodes when increased in primary tolerant recipients and blue nodes when increased in secondary tolerant recipients and connected with edges when correlated (Spearman correlation test, $P < 0.001$). Biological processes were analyzed with IPA and grouped in main modules, with gene names in green when increased in primary tolerant recipients (Fisher's exact test, $P < 0.01$). Upstream regulators were predicted with IPA and represented inside the dotted line circle ($P < 0.01$). (**F**) For the same set of 24 genes, pathways analysis was performed with IPA and ranked by −log(*P* value). BTG, B-cell translocation gene.

overrepresented in tolerant patients, as well as those involved in nucleobase-containing compounds catabolism (*NT5E*, which encodes CD73). The comparison of tolerant versus nontolerant patients identified 278 genes associated with outcome (data file S6). Correlation maps suggested that tolerance or absence of tolerance were related to two distinct gene expression profiles (Fig. 4C). Multiple biological processes linked to immune response regulation were associated with these genes, including adhesion and binding, migration, differentiation, survival, and homeostasis. Tolerance was associated with overexpression of genes associated with T cell differentiation (*IL23R* and *ICOS*) and with the ectoenzyme *NT5E* (ecto-5′-nucleotidase, CD73). CD73 catabolizes adenosine 5′-monophosphate (AMP) into adenosine, which exerts IS activity (*48*, *49*). Adenosine signaling has also been implicated in operational tolerance after liver transplantation (*50*, *51*). To confirm the role of CD73 in tolerant recipients, we assessed CD73 expression on immune subsets of donors and recipients using mass cytometry. This revealed that CD73 is down-regulated in nontolerant recipients in comparison to primary or secondary tolerant recipients, on total, transitional, naïve, and memory B cells (fig. S7). Canonical pathway enrichment analysis highlighted multiple changes in metabolic pathways but mainly showed that the absence of tolerance was associated with genes regulated by IFN-γ response, interleukin-10 (IL-10) up-regulation (Fig. 4C) and complement pathway activation (Fig. 4D). Last, as already observed in the comparison between donors and their primary tolerant recipients, the comparison between primary tolerant and secondary tolerant patients identified genes involved in cell cycle regulation as the main characteristic associated with primary tolerance (Fig. 4, E and F). To summarize, RNA sequencing analyses distinguished tolerant patients' transcriptomics profile. In particular, immune cells of tolerant patients exhibited a gene expression profile associated with multiple changes in immune function. Global overexpression of *NT5E* and its related expression of CD73 on B cells as confirmed by mass cytometry could bias nucleotide metabolism toward production of adenosine, which may contribute to the regulation of the immune response (*52*).

Metabolomic changes associated with tolerance highlight a central role of androgenic steroid metabolism

Immune responses in the context of GvHD are influenced by external factors such as circulating metabolites (*53*, *54*), including both host- and microbiota-derived metabolites. The comparison of tolerant and nontolerant recipients uncovered 91 metabolites that were differentially detected in plasma, six of them being microbiota-derived (Fig. 5A and data file S7). Metabolites of the androgenic and pregnenolone steroid pathways were the most increased compounds in tolerant recipients. Bile acids were overrepresented in nontolerant patients, as previously observed during acute GvHD (*55*) or in other inflammatory bowel diseases (*56*, *57*). Overrepresentation analysis also highlighted modifications associated with metabolism of amino acids and complex lipids, especially of phosphatidylcholine and sphingolipid metabolism (Fig. 5B). Consistent with the role of AMP catabolism into adenosine by CD73, we observed a significant increase in urate, the final metabolite of adenosine degradation, in tolerant recipients [fold change (FC) = 1.4, adjusted $P = 0.01$]. Among tolerant recipients, comparison of primary and secondary tolerant patients identified 25 differentially abundant metabolites (Fig. 5C and data file S8). Secondary tolerant patients exhibited higher concentrations of metabolites involved in phospholipids and tricarboxylic acid cycle (TCA) cycle (Fig. 5D). Last, feature selection uncovered 42 metabolites that were associated with tolerance in both cohorts. In addition to androgenic steroids metabolites, correlation maps revealed that tolerant recipients had higher amounts of metabolites that belonged to the phosphatidylcholine, amino acid, and ascorbate metabolism pathways (Fig. 5E). Among androgenic steroids, decreased dehydroepiandrosterone sulfate (DHEAS) (cohort 1, $P < 0.0001$; cohort 2, $P = 0.01$) and androstenediol (cohort 1 $P = 0.0008$; cohort 2, $P = 0.039$) were both associated with recipients' age. In summary, metabolomic analyses suggest an association between androgens and operational tolerance.

Integration of multiomics data describes the immune-metabolic network associated with operational tolerance

To get insights into the mechanisms involved in tolerance, we integrated phenotypic, transcriptomic, and metabolomic parameters. We built a correlation network linking clinical data and tolerance status (Fig. 6A). We calculated correlation between each principal component (PC) and clinical variables. For each of these PCs, the contribution of each data type was assessed and represented (Fig. 6B). PC1 and PC4 had the highest data variability that most correlated with the tolerance status and best discriminated tolerant from nontolerant recipients in both cohorts (Fig. 6C, fig. S8, and data file S9). A logistic regression confirmed this with statistically significant odds ratios (ORs) for both components (PC1: OR = 0.82, $P < 0.001$ and PC4: OR = 0.67, $P = 0.004$). Furthermore, the contribution of both PC1 and PC4 remained statistically significant (PC1: OR = 0.86, $P = 0.012$ and PC4: OR = 0.7, $P = 0.028$) after controlling for recipients' age, graft source, ATG treatment, and CMV status from the donor (table S2). Last, for each selected biological variable included in the integrative analysis, the relative contribution of age and gender was assessed by additional post hoc logistic regression models. In three metaclusters and 19 genes, representing 6% of the selected biological variables, the association with tolerance was no longer statistically significant after controlling for recipients 'age or gender (fig. S9). The biological variables that were used to build the principal components analysis (PCA) described in Fig. 6 (B and C) were then used to build a correlation map. Two main clusters of nodes were identified, associated with tolerance (blue dashed line) or absence of tolerance (orange dashed line), respectively (Fig. 6D).

In tolerant recipients, the androgenic steroid pathway was correlated with an increase in naïve $CD8^+$ T cells (metacluster 4) and multiple gene expression pathways (Fig. 6E). Both androgenic steroids and immune cells abundance in tolerant recipients correlated with genes involved in circadian control of gene expression, lipid metabolism, RORA [nuclear receptor retinoic acid receptor (RAR)-related orphan receptor A], and PPARA (peroxisome proliferator–activated receptor alpha) pathways (*NPAS2* and *ABCB4*). Multiple studies have stressed the role of the circadian clock as a core regulator for innate or adaptive immune response (*58*, *59*), and its disruption has been associated with T cell exhaustion in cancers (*60*). In addition, both naïve $CD8^+$ and DN T cells, as well as androgenic steroids, correlated with genes involved in pyrimidine and purine catabolism (*NT5E*). This suggests that lymphocyte homeostasis and regulatory subsets during tolerance might be linked to production of adenosine by the ecto-5′-nucleotidase CD73. Irrespective of recipient's gender, androgenic steroids were associated with tolerance in both recipients and donors (fig. S2G). Androgen steroids may affect the immune response by different mechanisms, including decreased antigen presentation by dendritic cells (*61*), impaired B cell lymphopoiesis (*62*), and improved negative thymic selection of T cells (*63*). In addition,

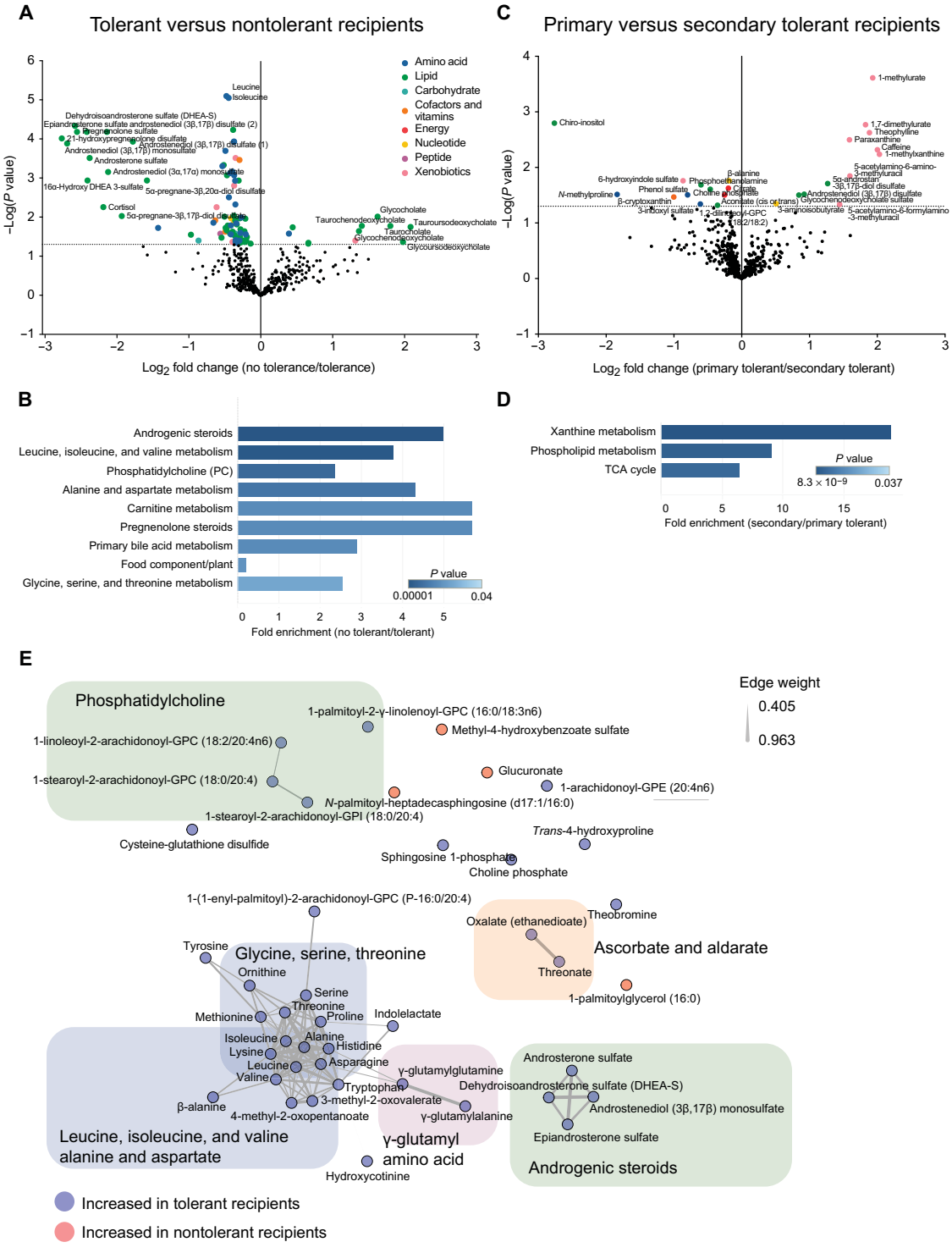

Fig. 5. Metabolomics profiling reveals differences between tolerant and nontolerant recipients. Metabolites that were detected in both cohorts ($n = 504$) with UPLC-MS/MS were compared with a Student's test, followed by a Benjamini-Hochberg correction. The volcano plot represents the variation of metabolites amount between tolerant and nontolerant recipients (**A**) or between primary and secondary tolerant recipients (**B**) according to the −log(*P* value) and colored according to metabolic pathways. Lists of the 90 and 24 significant metabolites, respectively, are available in data files S7 and S8. (**C** and **D**) Overrepresentation analysis of metabolic pathways is shown on the basis of metabolites identified by comparing tolerant and nontolerant recipients (C) or primary and secondary tolerant recipients (D), respectively, and ranked by *P* value (hypergeometric distribution). (**E**) The metabolites that were associated with tolerance or nontolerance in recipients were selected by multinomial regression models and feature selection with AUC > 0.9. A correlation map was built with these metabolites ($n = 42$) with nodes colored in blue when increased in tolerant recipients or red in nontolerant recipients and gray edges representing mean correlation rate in both cohort (Spearman correlation test, $P < 0.001$). Main metabolic pathways are represented as colored squares.

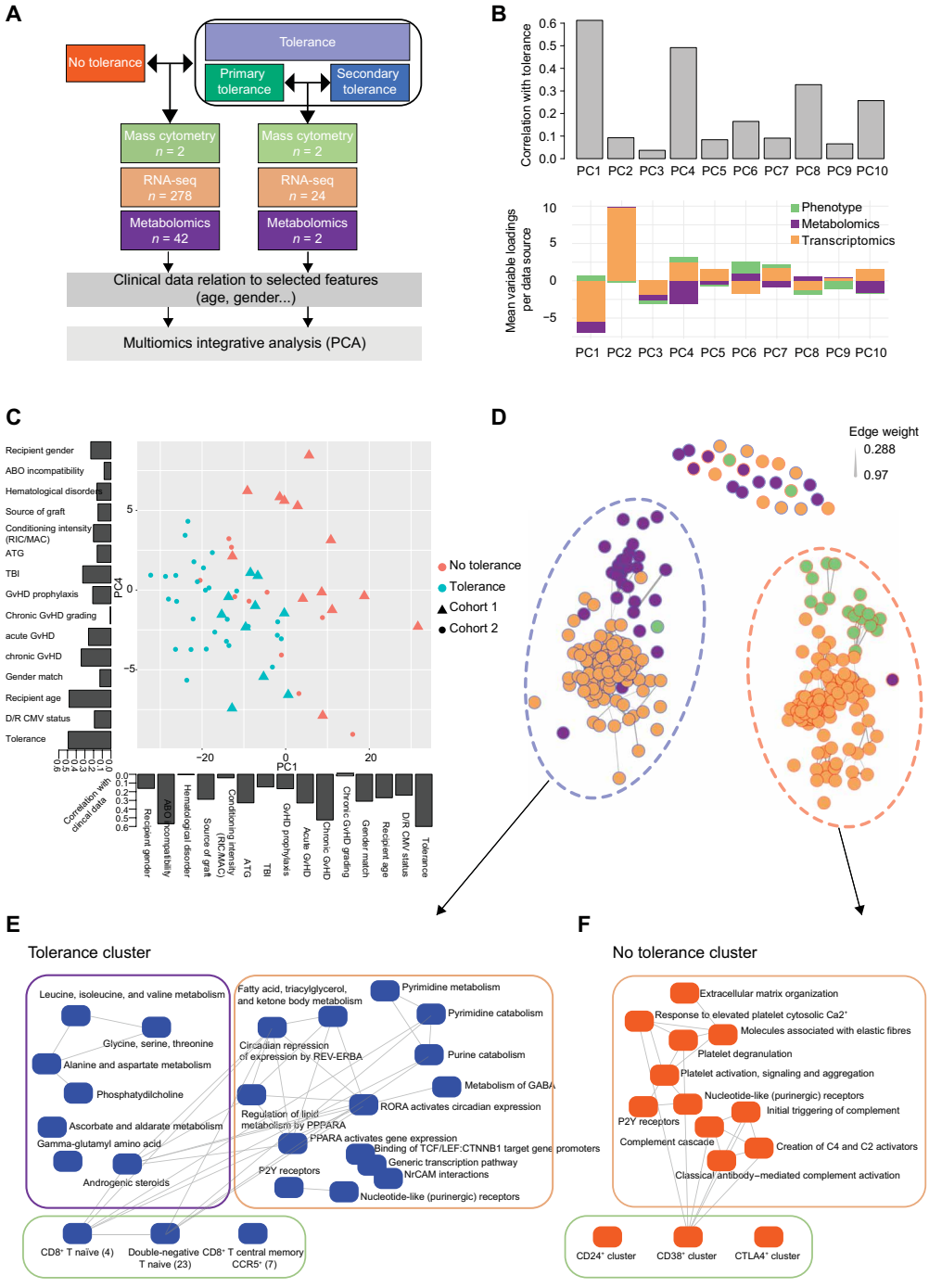

Fig. 6. The immune landscape differs between tolerant and nontolerant recipients as measured by integration of collected data. (**A**) Phenotypic, transcriptomic, and metabolomic variables that were identified by comparing tolerant and nontolerant recipients were integrated in a global analysis with clinical data using PCA. (**B**) For each PC, the correlation with outcome (tolerance or no tolerance) was measured and the contribution of each data type was measured. (**C**) The two PCs that were the most correlated with clinical outcome were used to represent patients from both cohorts (cohort 1, triangle; cohort 2, dot) according to their tolerance status (blue, tolerance; red, no tolerance). For each of the PCs, the correlation rate with clinical variables was represented as a histogram. TBI, total body irradiation; D/R , donor/recipient; RIC/MAC, reduced intensity conditioning regimen/myeloablative conditioning regimen. (**D**) A correlation map was built using each of the biological variables described inFigs. 3 to 5. Nodes are colored according to the type of data (phenotypic, $n = 24$; transcriptomics, $n = 278$; metabolomics, $n = 42$) and circled according to clinical outcome (blue if increased in tolerant recipients and red if increased in nontolerant recipients). Nodes are connected by edges representing mean correlation rate (Spearman correlation test, $P < 0.001$). (**E**) Nodes that were associated with tolerance were analyzed together to identify main metabolic pathways, immune subsets, and gene-associated biological processes [based on reactome database (*106*)]. Biological pathways were connected by edges when correlated together in both cohorts. GABA, γ-aminobutyric acid; CTNNB1, Catenin Beta 1; NrCAM, neuronal cell adhesion molecule. (**F**) The same representation was used to analyze biological features associated with the absence of tolerance, and biological pathways were connected by edges when correlated in both cohorts. Boxes are colored according to data type. See also fig. S7 representing the biological variables whose variations were associated with age or gender.

androgens could also bias T cell responses toward a T helper 2 (T_H2)–type response (*64*) and favor the development of regulatory T cells (*65*).

In nontolerant recipients, the CD38-expressing cluster was correlated with complement activation pathways (*C1QA*, *C1QB*, and *C1QC*), P2Y purinergic receptor signaling (*P2RY1*), and platelet activation (*SERPING1*) (Fig. 6F). These results suggest that the absence of tolerance in recipients may be linked to nicotinamide adenine dinucleotide (NAD^+) catabolism by CD38 expression on activated immune cells and signaling through the purinergic receptors P2Y (*66*).

Different cell cycle networks regulate primary versus secondary operational tolerance

To identify specific modifications in the immune landscape associated with primary tolerance, biological characteristics that distinguish primary versus secondary tolerant patients were lastly analyzed. Two PCs mainly correlated with primary or secondary tolerance (PC1 and PC2) (Fig. 7A) and best discriminated primary and secondary tolerance in both cohorts (Fig. 7B and data file S10). The correlation map mainly revealed a transcriptional network associated with primary tolerance (Fig. 7C) with up-regulation of multiple genes expression involved in cell cycle and DNA replication (*MKI67*, *PCLAF*, *E2F8*, *TOP2A*, and *UBE2C*) and of *AGMAT*, a gene coding for agmatinase, that converts the arginine-derived agmatine into the polyamine putrescine (Fig. 7D) (*67*). Polyamines regulate immune responses (*68*), negatively affect DNA replication and cell cycle progression (*69*–*71*), and reduce production of proinflammatory cytokines in monocytes and macrophages (*72*). Arginine metabolism is critical for T cell differentiation and survival (*73*, *74*). In contrast with primary tolerance, secondary tolerance was not associated with a specific transcriptomic signature but with the emergence of $CD38^+$ regulatory and central memory $CD4^+$ T cells subsets (Fig. 7D). These differences suggest that a specific immune-metabolic shift during primary tolerance could involve arginine metabolism and cell cycle regulation, whereas secondary tolerance that occurs after a first wave of allogeneic immune responses may rely on CD38 enhancement of regulatory cell activity.

DISCUSSION

Allo-HSCT is widely used in patients with hematologic disorders (*75*). Reaching a tolerant state after allo-HSCT remains the essential to avoid the devastating effect of GvHD. Here, we used an operational definition as described in the context of solid organ transplantation (*76*). Using two cohorts of patients who underwent allo-HSCT from an HLA-identical sibling donor, we describe how the immune system is reshaped 2 years after transplantation.

Vaccine responses have been previously used as a model to understand the evolving network between immune cells, genes expression profiles, and circulating metabolites (*77*). Elegant system analyses based on topological data analysis have previously demonstrated their ability to identify cellular perturbations associated with clinical outcomes after transplantation (*78*). Here, we extended this approach to the transcriptomic and metabolic levels to gain mechanistic insights into this network. These results revealed that tolerance is associated not only with the emergence of specific immune cell subsets but also with changes in the gene expression profile and in the metabolome, suggesting functional adaptation during tolerance. Our results reveal that immune system reshaping is complex, and biological pathways involved in immune tolerance deserve further analyses by functional assays or by validation in animal models.

The recognition by the donor's immune system of non–self-determinants in the host can lead to a potent allogeneic response that is responsible for GvHD after HSCT (*79*). In this study, restricting the population to patients with HLA-identical siblings avoided analyzing response against HLA molecules and allowed to directly compare the same immune system at baseline (healthy donor) and in an allogeneic environment. Furthermore, main clinical parameters that could influence the immune status were considered. Our study identified clinical parameters that were previously published as risk factor for acute or chronic GvHD, such as age, CMV status, graft source, and the use of ATG (*30*–*33*).

Integrated analysis revealed that the absence of operational tolerance after HSCT is largely associated with the expression of CD24, CTLA4, and CD38 on multiple immune cell subsets. CD38 expression on T cells has been previously proposed as a biomarker for acute (*80*, *81*) or chronic GvHD (*82*). CD38 catabolizes NAD^+ into adenosine 5′-diphosphate ribose (*83*). As a regulator of extracellular NAD^+ homeostasis, the CD38 activity regulates immune cell activation through not only cell metabolism reprogramming but also many other biological processes, such as circadian rhythm, DNA repair, or DNA methylation (*84*, *85*). Consistent with its ectoenzyme function, the CD38 cluster was correlated, in this study, with the expression of purinergic receptors, such as *P2RY1* and *P2RY10*. In murine models, the purinergic receptor P2X7R can sense danger signals such as adenosine 5′-triphosphate release and actuate proinflammatory events involved during GvHD (*86*). In addition, CD38 expression correlated with the expression of genes involved in both complement pathway and platelet activation. Chronic GvHD is associated with endothelial damages (*87*), and complement activation could be involved in GvHD-associated thrombotic microangiopathy (*88*, *89*). Complement activation may also contribute to T_H1 and T_H17 polarization in murine and human T cells during cutaneous GvHD (*90*, *91*). On the basis of integrated analyses, our results highlight a role for CD38 in persistent immune responses in nontolerant patients. This suggests that targeting CD38 or purinergic signaling may have therapeutic potential in GvHD, but further preclinical data are needed to confirm this hypothesis and to determine the optimal time point for targeting CD38 relative to GvHD onset. Furthermore, age-associated risk of GvHD may be explained by CD38-related decline of NAD^+ observed with aging (*83*, *92*).

Androgenic steroids correlated with immune cells and transcriptomic variations during tolerance. Recently, a low DHEAS concentration was associated with chronic GvHD in women, independently of conditioning, donor type, or recipients' age at transplant (*93*). Decreased androgens production has been associated with the altered immune function during aging (*94*), and sex steroids have been shown to affect thymopoiesis through modulation of Notch signaling (*95*) and to enhance negative selection of T cell by controlling autoimmune regulator expression and transforming growth factor–β production in the thymus (*63*, *96*). Although some androgenic steroids were globally associated with age in our study, they remained associated with tolerance status after controlling for age and gender. This suggests that they may contribute to tolerance, even if clinical association of age with tolerance could be, in part, biologically explained by the decrease in androgenic steroids with aging. In addition, it was recently suggested that human thymic functions not only decrease with age but is also lower in male than in female (*97*). Improved thymic functions in recipients may partially explain the correlation that we observed between androgenic steroids and increased naïve $CD8^+$ and regulatory DN T cells. Furthermore, androgenic steroids could also regulate

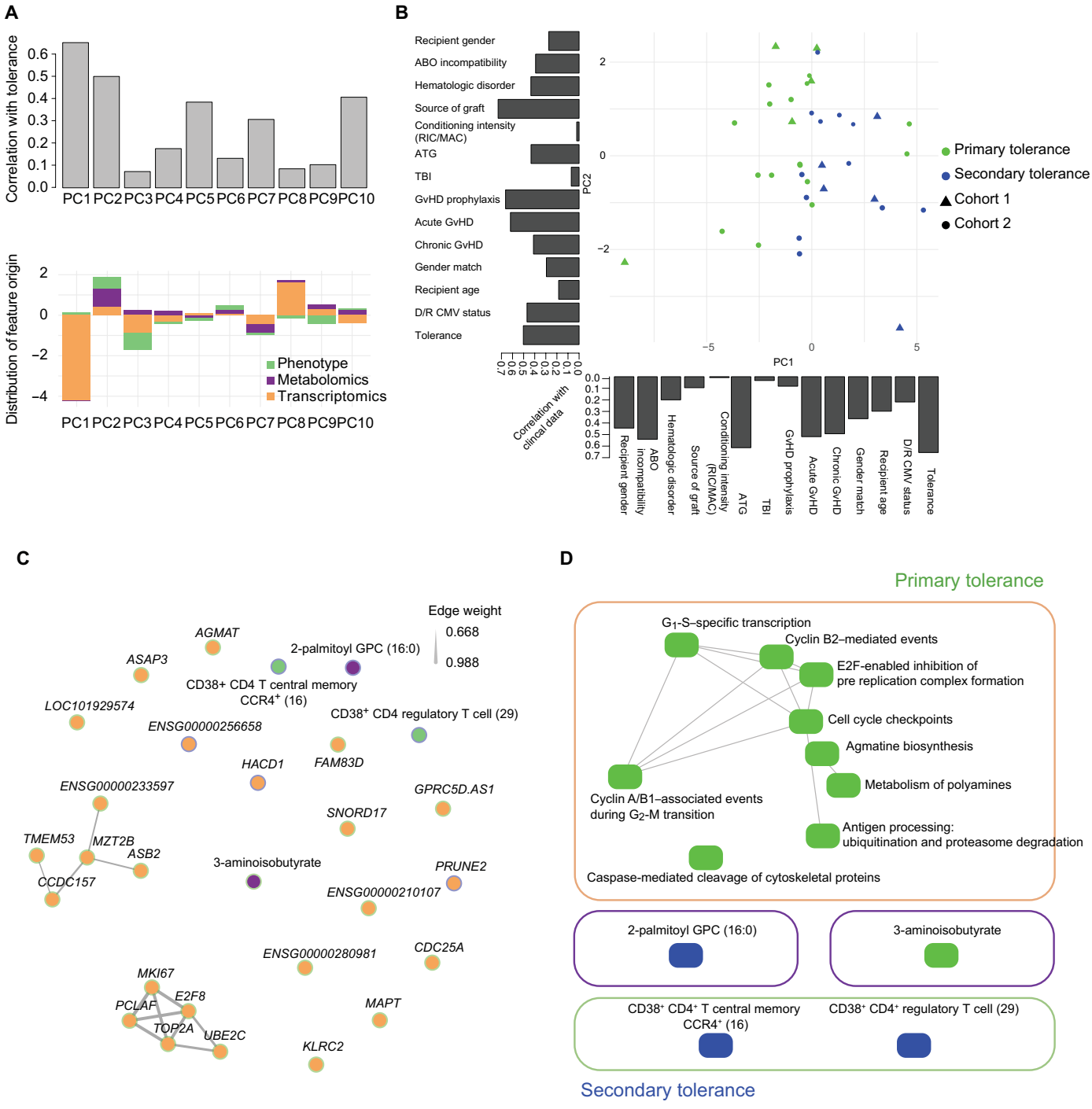

Fig. 7. The immune landscape differs between primary and secondary tolerant recipients as evaluated by integration of collected data. (**A**) PCA was performed using phenotypic ($n = 2$), transcriptomic ($n = 24$), and metabolomic ($n = 2$) features associated with primary or secondary tolerance. For each PC, correlation with primary or secondary tolerance was calculated, and the contribution of each data type was measured. (**B**) PC1 and PC2 were used to build a graph representing patients from both cohorts (triangle, cohort 1; dot, cohort 2) and colored according to their tolerance status (primary tolerant, green; secondary tolerant; blue). For each PC, correlations with clinical variable were represented in histograms. (**C**) A correlation map was built using each of the biological data used for PCA, with nodes colored according to data type (immune phenotype, green; transcriptomics, orange; metabolomics, violet) and circled according to clinical outcome (primary tolerant, green; secondary tolerant; blue). Mean correlations in both cohorts were calculated and represented as edges (Spearman correlation test, $P < 0.001$). (**D**) Nodes that were associated with primary (green) or secondary tolerance (blue) were analyzed together to identify main metabolic pathways, immune subsets, and gene-associated biological processes (based on reactome database (*106*)). Biological pathways were connected by edges when correlated together in both cohorts. Boxes are colored according to data type. GPC, Glycerophosphocholine.

peripheral immune cells, including T cell, B cell, and myeloid subsets (*98*). In tolerant patients, we found that the androgenic steroid pathway was correlated with expression of genes involved in purine and pyrimidine catabolism through the expression of *NT5E*, which encodes CD73. Production of adenosine from AMP metabolism by CD73 has a role in immune suppression by regulatory T cells (*99*) and inhibits both the innate and the adaptive response. Genes involved in the T cell factor 7 (TCF7)/Lymphoid enhancer binding factor 1 (LEF1) and Wnt signaling were associated with tolerance, suggesting that T cell stemness could play a major role in the regulation of alloimmune response. These later data are consistent with a previous experimental murine showing that the R-spondin1/Wnt interaction regulated systemic GvHD (*100*, *101*) and with recent data demonstrating that Dickkopf WNT Signaling Pathway Inhibitor 3 (DKK3), an inhibitor of Wnt pathway, was increased during chronic GvHD (*102*).

Few biological parameters, mainly transcriptomic variations, differed between primary and secondary tolerant recipients. Most of them involved genes that regulate cell cycle and were correlated with arginine and polyamine pathways. It has been previously demonstrated that arginine metabolism is a regulator of immune responses (*73*). Arginine conversion to polyamine could regulate cell division and contribute to immune suppression. Arginine can be directly converted to agmatine and polyamine by agmatinase, an enzyme coded by the gene *agmat* that we identified as being associated with primary tolerance and previously shown to be associated with regulation of immune response (*74*). Only two immune subsets distinguished primary and secondary tolerant patients, including $CD38^+CD4^+$ regulatory T cells. A previous study had suggested that CD38-related NAD^+ metabolism could prevent cell death in regulatory T cells (*103*), suggesting that the CD38 function during immune response is complex and depends on the cell subset where it is expressed.

Our study has several limitations. First, it was not designed to identify and validate biomarkers but rather to highlight biological pathways that may be used to modulate alloreactivity. Thus, biological variables that we identified cannot be used to predict tolerance or GvHD. Even if some of the variables that we had identified could be interesting biomarkers to predict or diagnose GvHD, it should be validated in prospective clinical trial with sequential sample from transplantation to GvHD occurrence. In addition, we cannot exclude that some other clinical parameters may have influenced biological parameters, especially exposure to IS drugs in the nontolerant group (but not in the tolerant one). Last, some of the biological mechanisms that we highlighted here would deserve to be confirmed using functional approach, especially through the use of animal models.

In summary, integration of whole biological data shed light on how biological variations after allo-HSCT can shape the immune landscape toward tolerance and could be possibly influenced by age. The balance of the immune signal from an activated state, associated with expression of the ectoenzyme CD38, to a steady state, associated with CD73-related production of adenosine, may be important in the regulation of this network. These results provide an overview of how immunometabolic network can lead to immune tolerance after transplantation and highlight therapeutic targets that may improve allo-HSCT outcome.

MATERIALS AND METHODS

Study design

This study includes recipients (and their HLA-identical sibling donors) who underwent a first allo-HSCT. Two cohorts have been analyzed: one monocentric cohort (local cohort 1, 41 couples) and one multicentric cohort (national cohort 2, 69 couples). The monocentric cohort included patients who underwent allo-HSCT at Saint Louis Hospital (Paris, France). The multicentric cohort included patients transplanted in one of the 33 French national transplant centers involved in CRYOSTEM Consortium, funded under the French government's National Investment Program (Investissement d'Avenir). Inclusion criteria were adult patients (more than 18 years old), with an HLA-identical sibling donor. Patients with HIV or Human T cell leukemia virus coinfection were excluded. Our objectives were to include at least 40 patients per cohort with an expected GvHD incidence of 40%. All patients gave their written consent for clinical research. This noninterventional research study with no additional clinical procedure was carried out in accordance with the Declaration of Helsinki. Data analyses were carried out using a database with all patient identifiers removed. This study was declared to the CNIL (Commission National Informatique et Liberté, number KoT1175225K) and was approved by the local ethic committee and Institutional Review Board (CPP Ile de France IV, IRB number 00003835, reference number 2014/37NICB). This project has been registered on clinicaltrial.gov under the accession number NCT02319226. Further information about patient characteristics, sampling, and outcomes can be found in the Supplementary Materials and in table S1.

Antibodies and antibody labeling

Clone, metal tags, and providers for each antibody used in this study are available in table S3. Metal labeling of the antibodies anti-human CD19, CCR5, CD27, CD45RA, CD95, immunoglobulin D, and LAG-3 was done using the Maxpar Antibody Conjugation Kit by Fluidigm per the manufacturer's instructions. Anti-human IL-10 metal labeling was performed using the SiteClick Qdot 800 Antibody Labeling Kit (Life Technologies) per the manufacturer's instructions.

Antibody staining

Cryopreserved PBMCs were thawed and washed with prewarmed RPMI 1640 supplemented with fetal bovine serum (FBS) in a 50%/50% solution. Two hundred and fifty units of Pierce universal nuclease for cell lysis (Thermo Fisher Scientific) was added to each sample followed by 30 min of incubation at 37°C. Cells were washed twice with prewarmed RPMI 1640 and stained afterward for viability with Cisplatin Cell-ID (Fluidigm) at a 0.5 μM concentration. Cells were washed and place in staining buffer (Fluidigm), followed by two staining steps: one at 37°C and the other at 4°C, each with 30-min incubation (see table S2 for details). Cells were fixed in 2% paraformaldehyde (PFA) and permeabilized with perm buffer (eBioscience) before intracellular staining for 30 min. Cells were then put in a solution of intercalator-iridium (Fluidigm) diluted 1:6000 in 2% PFA overnight.

Mass cytometry acquisition

A large-scale mass cytometry analysis was performed using 38 phenotypic and functional markers, allowing the identification of populations and subpopulations of $CD4^+$ and $CD8^+$ T cells, B cells, myeloid cells, and NK cells. Identification of nucleated and alive cells was done with intercalator-iridium (Fluidigm) and Cisplatin Cell-ID (Fluidigm) markers, respectively. Before mass cytometry acquisition, cells were washed twice in staining buffer and twice in Maxpar water (Fluidigm). Cells were then resuspended in Maxpar water (Fluidigm) at 1 million cells/ml, mixed with 10% of equalization beads (Fluidigm)

and passed through a cell strainer cap with 35-μm pores (BD Biosciences) immediately before acquisition.

RNA extraction and sequencing

Cryopreserved PBMCs were thawed and washed with prewarmed RPMI 1640 and 50% FBS. Total RNA extraction was performed using Promega Maxwell technology (simply RNA tissue kit, AS1340) according to the manufacturer's protocol. RNA samples concentration was then measured using a NanoDrop 2000 Spectrophotometer, and aliquots with a minimal concentration of 20 ng/μl were diluted. The quality of RNA was evaluated by a NanoDrop Spectrophotometer and Bioanalyzer (Agilent Technologies).

Total stranded RNA sequencing was performed by the Centre National de Recherche en Génomique Humaine (Institut de Biologie François Jacob). A complete RNA quality control on each sample (quantification in duplicate on a NanoDrop 8000 Spectrophotometer and RNA 6000 Nano LabChip analysis on Bioanalyzer from Agilent) was done, and only samples with sufficient quality were selected for further analysis: median RNA integrity number of 8.2 for cohort 1 (5.7 to 9.2 range) and 7.8 for cohort 2 (5.9 to 9.2 range). Libraries have been prepared using the TruSeq Stranded Total RNA Gold Kit from Illumina, which removes both cytoplasmic and mitochondrial ribosomal RNA as a first step of library preparation. An input of 200 ng total RNA was used for all samples, and libraries were prepared on an automated platform, according to the manufacturer's instructions. Library quality has been checked by LabGx (PerkinElmer) analysis for profile analysis and quantification, and sample libraries have then been pooled before sequencing to reach the expected sequencing depth. Sequencing has been performed on an Illumina HiSeq4000 as paired-end 100–base pair reads using Illumina sequencing reagents. Libraries were generally pooled by four samples per lane, corresponding, on average, to 70 to 90 million sequenced fragments (or 140 to 180 million total reads).

Plasma metabolomics using MS

Plasma aliquots were sent to Metabolon. The metabolomics data acquisition using MS (UPLC-MS/MS Acquity), quality assurance and quality control, compound identification, and quantification were performed as previously described (*55*). Details on metabolomics can be found in Supplementary Methods.

Statistical analysis

Univariate analysis of clinical variables in both cohorts combined was performed using a Kruskal-Wallis test for continuous variables or a chi-squared test for categorical variables. All *P* values were adjusted using a Benjamini-Hochberg correction for multiple testing. To assess the relative associations of clinical variables with tolerance, a multivariate multinomial logistic regression model was built with primary tolerance as reference level using the nnet R package on Comprehensive R Archive Network (CRAN). For comparison of donors and recipients, gene expression values in donors and recipients were centered and scaled. Recipients' values were then subtracted to donors' values per couple to determine how much the expression of a gene changed between the time of graft and the 2-year time point in each donor-recipient couple. Nonparametric paired Wilcoxon ranked tests were performed to compare donors and recipients. A nonparametric Mann-Whitney *U* test was performed for comparison of unpaired samples, and a Benjamini-Hochberg correction for multiple testing was applied to calculate a *P* value associated with the false discovery rate. Biological variables were only retained if they were statistically significant in both cohorts.

For feature selection, two logistic regression models were built in which patients' tolerance versus nontolerance and patient's primary versus secondary tolerance were used as outcome, and the features (such as biological variables obtained from mass cytometry, RNA sequencing, or metabolomics) were used as predictors. These models were built using the stats R package on CRAN, and the average AUC for the two pairwise outcome comparisons was extracted using the pROC R package on CRAN. Next, the feature was permuted 1000 times, and the corresponding models were updated, resulting in a permutation distribution of AUCs. If the quantile associated with the AUC of the original feature exceeded 90% of the permuted AUCs (qAUC > 0.9), then the feature was selected. To verify that the association between tolerance and the selected biological features could not solely be explained by clinical variables, logistic regression models for biological parameters were expanded with age and gender matching as covariates of no interest. Forest plots were built to represent the OR with 95% confidence interval of tolerance over none associated with a one unit increase in the variable. Only biological variables that were selected independently in both cohorts were retained and used for correlation analysis.

To identify correlated features, Spearman correlation tests were performed between the biological parameters that have been selected in both cohorts and exhibited the same variation between groups. Only correlations with an associated $P < 0.001$ in both cohorts were kept. These correlations were represented in graphs, where the width of an edge between two variables corresponds to the mean of the correlation between these two variables in both cohorts.

The biological parameters that were selected by feature selection in the three data modalities (metabolomics, immunophenotypic, and transcriptomics) were used to build two integrative analyses in tolerant versus nontolerant recipients and in primary versus secondary tolerant recipients. To do so, we could only use the data from patients for which these three types of data had been generated. This resulted in 23 donor-recipient couples in cohort 1 and 38 couples in cohort 2 for the comparison of tolerant and nontolerant couples. In the comparison of primary versus secondary patients, the integrative analysis was done on 10 donor-recipient couples in cohort 1 and 27 couples in cohort 2. Because the features from the different data modalities had all been log-transformed, centered, and scaled, these features could directly be integrated into one model. We thus performed PCA on all these biological variables taken together. The correlation between each PC and clinical variables was calculated. PCs that had the highest data variability that most correlated with the tolerance were selected. For these PCs, the correlation with other clinical variables was calculated, and logistic regression models were built with tolerance as outcome and the PCs as predictors. To verify the independent contribution of the PCs, the model was expanded with clinical variables associated with tolerance. Last, to assess the relative contribution of age and gender in each selected biological characteristic included in the integrative analysis, additional post hoc logistic regression models including age and gender were performed. The variables that were used to build the PCA were then used to build a correlation map.

For metabolomics, metabolites that were identified by statistical analysis were then used to build an overrepresentation analysis. Enrichment (*E*) was calculated by considering the number of metabolites identified in each pathway (*k*), the total number of metabolites

identified (n), the number of metabolites in each pathway (m), and the total number of metabolites used for analysis (M) as follow: $E = (k/m)/((n-k)/(N-m))$. For each pathway, P values were determined by calculation of the hypergeometric distribution. For transcriptomics, two enrichment analyses were conducted with genes identified by statistical analysis. Canonical pathways (such as signaling and metabolic pathways) and biological processes were analyzed with ingenuity pathway analysis (IPA) (QIAGEN, v51963813) and Gene Ontology atlas (*104*, *105*). Statistical significance was calculated with Fisher's exact test. For final integrative analysis, biological processes associated with selected genes were analyzed using reactome database (*106*).

SUPPLEMENTARY MATERIALS

www.science.org/doi/10.1126/scitranslmed.abg3083
Methods
Figs. S1 to S9
Tables S1 to S3
Data files S1 to S10
References (*110*–*115*)

View/request a protocol for this paper from *Bio-protocol*.

REFERENCES AND NOTES

1. R. E. Billingham, L. Brent, P. B. Medawar, Actively acquired tolerance of foreign cells. *Nature* **172**, 603–606 (1953).
2. J. A. Bluestone, M. Anderson, Tolerance in the age of immunotherapy. *N. Engl. J. Med.* **383**, 1156–1166 (2020).
3. M. S. Anderson, M. A. Su, AIRE expands: New roles in immune tolerance and beyond. *Nat. Rev. Immunol.* **16**, 247–258 (2016).
4. A. N. Theofilopoulos, D. H. Kono, R. Baccala, The multiple pathways to autoimmunity. *Nat. Immunol.* **18**, 716–724 (2017).
5. J. Stolp, M. Zaitsu, K. J. Wood, in *Immunological Tolerance: Methods and Protocols*, A. S. Boyd, Ed. (Springer, 2019), pp. 159–180.
6. T. E. Starzl, N. Murase, A. J. Demetris, M. Trucco, K. Abu-Elmagd, E. A. Gray, B. Eghtesad, R. Shapiro, A. Marcos, J. J. Fung, Lessons of organ-induced tolerance learned from historical clinical experience. *Transplantation* **77**, 926–929 (2004).
7. J. Lerut, A. Sanchez-Fueyo, An appraisal of tolerance in liver transplantation. *Am. J. Transplant.* **6**, 1774–1780 (2006).
8. G. Roussey-Kesler, M. Giral, A. Moreau, J.-F. Subra, C. Legendre, C. Noël, E. Pillebout, S. Brouard, J.-P. Soulillou, Clinical operational tolerance after kidney transplantation. *Am. J. Transplant.* **6**, 736–746 (2006).
9. S. Brouard, A. Pallier, K. Renaudin, Y. Foucher, R. Danger, A. Devys, A. Cesbron, C. Guillot-Guegen, J. Ashton-Chess, S. L. Roux, J. Harb, G. Roussey, J.-F. Subra, F. Villemain, C. Legendre, F. J. Bemelman, G. Orlando, A. Garnier, H. Jambon, H. L. M. D. Sagazan, L. Braun, C. Noël, E. Pillebout, M.-C. Moal, C. Cantarell, A. Hoitsma, M. Ranbant, A. Testa, J.-P. Soulillou, M. Giral, The natural history of clinical operational tolerance after kidney transplantation through twenty-seven cases. *Am. J. Transplant.* **12**, 3296–3307 (2012).
10. M. Martínez-Llordella, I. Puig-Pey, G. Orlando, M. Ramoni, G. Tisone, A. Rimola, J. Lerut, D. Latinne, C. Margarit, I. Bilbao, S. Brouard, M. Hernández-Fuentes, J.-P. Soulillou, A. Sánchez-Fueyo, Multiparameter immune profiling of operational tolerance in liver transplantation. *Am. J. Transplant.* **7**, 309–319 (2007).
11. M. Chesneau, A. Pallier, F. Braza, G. Lacombe, S. Le Gallou, D. Baron, M. Giral, R. Danger, P. Guerif, H. Aubert-Wastiaux, A. Néel, L. Michel, D.-A. Laplaud, N. Degauque, J.-P. Soulillou, K. Tarte, S. Brouard, Unique B cell differentiation profile in tolerant kidney transplant patients. *Am. J. Transplant.* **14**, 144–155 (2014).
12. K. A. Newell, A. Asare, A. D. Kirk, T. D. Gisler, K. Bourcier, M. Suthanthiran, W. J. Burlingham, W. H. Marks, I. Sanz, R. I. Lechler, M. P. Hernandez-Fuentes, L. A. Turka, V. L. Seyfert-Margolis, Identification of a B cell signature associated with renal transplant tolerance in humans. *J. Clin. Invest.* **120**, 1836–1847 (2010).
13. A. Pallier, S. Hillion, R. Danger, M. Giral, M. Racapé, N. Degauque, E. Dugast, J. Ashton-Chess, S. Pettré, J. J. Lozano, R. Bataille, A. Devys, A. Cesbron-Gautier, C. Braudeau, C. Larrose, J.-P. Soulillou, S. Brouard, Patients with drug-free long-term graft function display increased numbers of peripheral B cells with a memory and inhibitory phenotype. *Kidney Int.* **78**, 503–513 (2010).
14. P. Sagoo, E. Perucha, B. Sawitzki, S. Tomiuk, D. A. Stephens, P. Miqueu, S. Chapman, L. Craciun, R. Sergeant, S. Brouard, F. Rovis, E. Jimenez, A. Ballow, M. Giral, I. Rebollo-Mesa, A. Le Moine, C. Braudeau, R. Hilton, B. Gerstmayer, K. Bourcier, A. Sharif, M. Krajewska, G. M. Lord, I. Roberts, M. Goldman, K. J. Wood, K. Newell, V. Seyfert-Margolis, A. N. Warrens, U. Janssen, H.-D. Volk, J.-P. Soulillou, M. P. Hernandez-Fuentes, R. I. Lechler, Development of a cross-platform biomarker signature to detect renal transplant tolerance in humans. *J. Clin. Invest.* **120**, 1848–1861 (2010).
15. H. M. Silva, M. C. S. Takenaka, P. M. M. Moraes-Vieira, S. M. Monteiro, M. O. Hernandez, W. Chaara, A. Six, F. Agena, P. Sesterheim, F. M. Barbé-Tuana, D. Saitovitch, F. Lemos, J. Kalil, V. Coelho, Preserving the B-cell compartment favors operational tolerance in human renal transplantation. *Mol. Med.* **18**, 733–743 (2012).
16. J. Stolp, L. A. Turka, K. J. Wood, B cells with immune-regulating function in transplantation. *Nat. Rev. Nephrol.* **10**, 389–397 (2014).
17. T. Kawai, A. B. Cosimi, T. R. Spitzer, N. Tolkoff-Rubin, M. Suthanthiran, S. L. Saidman, J. Shaffer, F. I. Preffer, R. Ding, V. Sharma, J. A. Fishman, B. Dey, D. S. C. Ko, M. Hertl, N. B. Goes, W. Wong, W. W. Williams, R. B. Colvin, M. Sykes, D. H. Sachs, HLA-mismatched renal transplantation without maintenance immunosuppression. *N. Engl. J. Med.* **358**, 353–361 (2008).
18. J. Zuber, M. Sykes, Mechanisms of mixed chimerism-based transplant tolerance. *Trends Immunol.* **38**, 829–843 (2017).
19. J. R. Leventhal, M. J. Elliott, E. S. Yolcu, L. D. Bozulic, D. J. Tollerud, J. M. Mathew, I. Konieczna, M. G. Ison, J. Galvin, J. Mehta, M. D. Badder, M. M. I. Abecassis, J. Miller, L. Gallon, S. T. Ildstad, Immune reconstitution/immunocompetence in recipients of kidney plus hematopoietic stem/facilitating cell transplants. *Transplantation* **99**, 288–298 (2015).
20. J. D. Scandling, S. Busque, J. A. Shizuru, R. Lowsky, R. Hoppe, S. Dejbakhsh-Jones, K. Jensen, A. Shori, J. A. Strober, P. Lavori, B. B. Turnbull, E. G. Engleman, S. Strober, Chimerism, graft survival, and withdrawal of immunosuppressive drugs in hla matched and mismatched patients after living donor kidney and hematopoietic cell transplantation. *Am. J. Transplant.* **15**, 695–704 (2015).
21. P. Matzinger, T. Kamala, Tissue-based class control: The other side of tolerance. *Nat. Rev. Immunol.* **11**, 221–230 (2011).
22. S.-R. Wu, P. Reddy, Tissue tolerance: A distinct concept to control acute GVHD severity. *Blood* **129**, 1747–1752 (2017).
23. E. A. Copelan, Hematopoietic stem-cell transplantation. *N. Engl. J. Med.* **354**, 1813–1826 (2006).
24. O. Ringdén, S. Z. Pavletic, C. Anasetti, A. J. Barrett, T. Wang, D. Wang, J. H. Antin, P. D. Bartolomeo, B. J. Bolwell, C. Bredeson, M. S. Cairo, R. P. Gale, V. Gupta, T. Hahn, G. A. Hale, J. Halter, M. Jagasia, M. R. Litzow, F. Locatelli, D. I. Marks, P. L. McCarthy, M. J. Cowan, E. W. Petersdorf, J. A. Russell, G. J. Schiller, H. Schouten, S. Spellman, L. F. Verdonck, J. R. Wingard, M. M. Horowitz, M. Arora, The graft-versus-leukemia effect using matched unrelated donors is not superior to HLA-identical siblings for hematopoietic stem cell transplantation. *Blood* **113**, 3110–3118 (2009).
25. R. S. Negrin, Graft-versus-host disease versus graft-versus-leukemia. *Hematology Am. Soc. Hematol. Educ. Program* **2015**, 225–230 (2015).
26. R. Zeiser, B. R. Blazar, Pathophysiology of chronic graft-versus-host disease and therapeutic targets. *N. Engl. J. Med.* **377**, 2565–2579 (2017).
27. R. Zeiser, B. R. Blazar, Acute graft-versus-host disease. *N. Engl. J. Med.* **378**, 586 (2018).
28. S. G. Holtan, T. E. DeFor, A. Lazaryan, N. Bejanyan, M. Arora, C. G. Brunstein, B. R. Blazar, M. L. MacMillan, D. J. Weisdorf, Composite end point of graft-versus-host disease-free, relapse-free survival after allogeneic hematopoietic cell transplantation. *Blood* **125**, 1333–1338 (2015).
29. S. Van Gassen, B. Callebaut, M. J. Van Helden, B. N. Lambrecht, P. Demeester, T. Dhaene, Y. Saeys, FlowSOM: Using self-organizing maps for visualization and interpretation of cytometry data. *Cytometry A* **87**, 636–645 (2015).
30. J. Pidala, M. Martens, C. Anasetti, J. Carreras, M. Horowitz, S. J. Lee, J. Antin, C. Cutler, B. Logan, Factors associated with successful discontinuation of immune suppression after allogeneic hematopoietic cell transplantation. *JAMA Oncol.* **6**, e192974 (2020).
31. C. Anasetti, B. R. Logan, S. J. Lee, E. K. Waller, D. J. Weisdorf, J. R. Wingard, C. S. Cutler, P. Westervelt, A. Woolfrey, S. Couban, G. Ehninger, L. Johnston, R. T. Maziarz, M. A. Pulsipher, D. L. Porter, S. Mineishi, J. M. McCarty, S. P. Khan, P. Anderlini, W. I. Bensinger, S. F. Leitman, S. D. Rowley, C. Bredeson, S. L. Carter, M. M. Horowitz, D. L. Confer; Blood and Marrow Transplant Clinical Trials Network, Peripheral-blood stem cells versus bone marrow from unrelated donors. *N. Engl. J. Med.* **367**, 1487–1496 (2012).
32. S. Arai, M. Arora, T. Wang, S. R. Spellman, W. He, D. R. Couriel, A. Urbano-Ispizua, C. S. Cutler, A. A. Bacigalupo, M. Battiwalla, M. E. Flowers, M. B. Juckett, S. J. Lee, A. W. Loren, T. R. Klumpp, S. E. Prockup, O. T. H. Ringdén, B. N. Savani, G. Socié, K. R. Schultz, T. Spitzer, T. Teshima, C. N. Bredeson, D. A. Jacobsohn, R. J. Hayashi, W. R. Drobyski, H. A. Frangoul, G. Akpek, V. T. Ho, V. A. Lewis, R. P. Gale, J. Koreth, N. J. Chao, M. D. Aljurf, B. W. Cooper, M. J. Laughlin, J. W. Hsu, P. Hematti, L. F. Verdonck, M. M. Solh, M. Norkin, V. Reddy, R. Martino, S. Gadalla, J. D. Goldberg, P. L. McCarthy, J. A. Pérez-Simón, N. Khera, I. D. Lewis, Y. Atsuta, R. F. Olsson, W. Saber, E. K. Waller, D. Blaise, J. A. Pidala, P. J. Martin, P. Satwani, M. Bornhäuser, Y. Inamoto, D. J. Weisdorf, M. M. Horowitz, S. Z. Pavletic; Graft-vs-Host Disease Working Committee of the CIBMTR, Increasing incidence of chronic graft-versus-host disease in allogeneic transplantation: A report from the Center for International Blood and Marrow Transplant Research. *Biol. Blood Marrow Transplant.* **21**, 266–274 (2015).

33. J. Finke, W. A. Bethge, C. Schmoor, H. D. Ottinger, M. Stelljes, A. R. Zander, L. Volin, T. Ruutu, D. A. Heim, R. Schwerdtfeger, K. Kolbe, J. Mayer, J. A. Maertens, W. Linkesch, E. Holler, V. Koza, M. Bornhäuser, H. Einsele, H.-J. Kolb, H. Bertz, M. Egger, O. Grishina, G. Socié; ATG-Fresenius Trial Group, Standard graft-versus-host disease prophylaxis with or without anti-T-cell globulin in haematopoietic cell transplantation from matched unrelated donors: A randomised, open-label, multicentre phase 3 trial. *Lancet Oncol.* **10**, 855–864 (2009).
34. A. Kalra, T. Williamson, A. Daly, M. L. Savoie, D. A. Stewart, F. Khan, J. Storek, Impact of donor and recipient cytomegalovirus serostatus on outcomes of antithymocyte globulin-conditioned hematopoietic cell transplantation. *Biol. Blood Marrow Transplant.* **22**, 1654–1663 (2016).
35. C. Baron, R. Somogyi, L. D. Greller, V. Rineau, P. Wilkinson, C. R. Cho, M. J. Cameron, D. J. Kelvin, P. Chagnon, D.-C. Roy, L. Busque, R.-P. Sékaly, C. Perreault, Prediction of graft-versus-host disease in humans by donor gene-expression profiling. *PLoS Med.* **4**, e23 (2007).
36. G. Das, M. M. Augustine, J. Das, K. Bottomly, P. Ray, A. Ray, An important regulatory role for $CD4^+CD8\alpha\alpha$ T cells in the intestinal epithelial layer in the prevention of inflammatory bowel disease. *PNAS* **100**, 5324–5329 (2003).
37. B. S. Reis, A. Rogoz, F. A. Costa-Pinto, I. Taniuchi, D. Mucida, Mutual expression of the transcription factors Runx3 and ThPOK regulates intestinal $CD4^+$ T cell immunity. *Nat. Immunol.* **14**, 271–280 (2013).
38. L. Van Kaer, W. A. S. Rabacal, H. M. Scott Algood, V. V. Parekh, D. Olivares-Villagómez, In vitro induction of regulatory $CD4^+CD8\alpha^+$ T cells by TGF-β, IL-7 and IFN-γ. *PLOS ONE* **8**, e67821 (2013).
39. K. Fischer, S. Voelkl, J. Heymann, G. K. Przybylski, K. Mondal, M. Laumer, L. Kunz-Schughart, C. A. Schmidt, R. Andreesen, A. Mackensen, Isolation and characterization of human antigen-specific $TCR\alpha\beta^+$ $CD4^-CD8^-$ double-negative regulatory T cells. *Blood* **105**, 2828–2835 (2005).
40. S. Strober, S. Dejbachsh-Jones, P. V. Vlasselaer, G. Duwe, S. Salimi, J. P. Allison, Cloned natural suppressor cell lines express the CD3+CD4-CD8- surface phenotype and the alpha, beta heterodimer of the T cell antigen receptor. *J. Immunol.* **143**, 1118–1122 (1989).
41. Z. X. Zhang, L. Yang, K. J. Young, B. DuTemple, L. Zhang, Identification of a previously unknown antigen-specific regulatory T cell and its mechanism of suppression. *Nat. Med.* **6**, 782–789 (2000).
42. T. Haug, M. Aigner, M. M. Peuser, C. D. Strobl, K. Hildner, D. Mougiakakos, H. Bruns, A. Mackensen, S. Völkl, Human double-negative regulatory T-cells induce a metabolic and functional switch in effector T-cells by suppressing mtor activity. *Front. Immunol.* **10**, 883 (2019).
43. A. J. Ligocki, J. Y. Niederkorn, Advances on non-CD4 + Foxp3+ T regulatory cells: CD8+, type 1, and double negative T regulatory cells in organ transplantation. *Transplantation* **99**, 1553–1559 (2015).
44. L. van de Laar, W. Saelens, S. De Prijck, L. Martens, C. L. Scott, G. Van Isterdael, E. Hoffmann, R. Beyaert, Y. Saeys, B. N. Lambrecht, M. Guilliams, Yolk sac macrophages, fetal liver, and adult monocytes can colonize an empty niche and develop into functional tissue-resident macrophages. *Immunity* **44**, 755–768 (2016).
45. M. Sade-Feldman, K. Yizhak, S. L. Bjorgaard, J. P. Ray, C. G. de Boer, R. W. Jenkins, D. J. Lieb, J. H. Chen, D. T. Frederick, M. Barzily-Rokni, S. S. Freeman, A. Reuben, P. J. Hoover, A.-C. Villani, E. Ivanova, A. Portell, P. H. Lizotte, A. R. Aref, J.-P. Eliane, M. R. Hammond, H. Vitzthum, S. M. Blackmon, B. Li, V. Gopalakrishnan, S. M. Reddy, Z. A. Cooper, C. P. Paweletz, D. A. Barbie, A. Stemmer-Rachamimov, K. T. Flaherty, J. A. Wargo, G. M. Boland, R. J. Sullivan, G. Getz, N. Hacohen, Defining T cell states associated with response to checkpoint immunotherapy in melanoma. *Cell* **175**, 998–1013.e20 (2018).
46. I. Siddiqui, K. Schaeuble, V. Chennupati, S. A. Fuertes Marraco, S. Calderon-Copete, D. Pais Ferreira, S. J. Carmona, L. Scarpellino, D. Gfeller, S. Pradervand, S. A. Luther, D. E. Speiser, W. Held, Intratumoral $Tcf1^+PD\text{-}1^+CD8^+$ T cells with stem-like properties promote tumor control in response to vaccination and checkpoint blockade immunotherapy. *Immunity* **50**, 195–211.e10 (2019).
47. K. E. Yost, A. T. Satpathy, D. K. Wells, Y. Qi, C. Wang, R. Kageyama, K. L. McNamara, J. M. Granja, K. Y. Sarin, R. A. Brown, R. K. Gupta, C. Curtis, S. L. Bucktrout, M. M. Davis, A. L. S. Chang, H. Y. Chang, Clonal replacement of tumor-specific T cells following PD-1 blockade. *Nat. Med.* **25**, 1251–1259 (2019).
48. M. G. Costales, M. S. Alam, C. Cavanaugh, K. M. Williams, Extracellular adenosine produced by ecto-5′-nucleotidase (CD73) regulates macrophage pro-inflammatory responses, nitric oxide production, and favors Salmonella persistence. *Nitric Oxide* **72**, 7–15 (2018).
49. C. Silva-Vilches, S. Ring, J. Schrader, B. E. Clausen, H.-C. Probst, F. Melchior, H. Schild, A. Enk, K. Mahnke, Production of extracellular adenosine by $CD73^+$ dendritic cells is crucial for induction of tolerance in contact hypersensitivity reactions. *J. Invest. Dermatol.* **139**, 541–551 (2019).
50. A. Baroja-Mazo, B. Revilla-Nuin, Á. de Bejar, L. Martínez-Alarcón, J. I. Herrero, A. El-Tayeb, C. E. Müller, P. Aparicio, P. Pelegrín, J. A. Pons, Extracellular adenosine reversibly inhibits the activation of human regulatory T cells and negatively influences the achievement of the operational tolerance in liver transplantation. *Am. J. Transplant.* **19**, 48–61 (2019).
51. E. Castillo-Leon, S. Dellepiane, P. Fiorina, ATP and T-cell-mediated rejection. *Curr. Opin. Organ Transplant.* **23**, 34–43 (2018).
52. H. Kaku, K. F. Cheng, Y. Al-Abed, T. L. Rothstein, A novel mechanism of B cell–mediated immune suppression through CD73 expression and adenosine production. *J. Immunol.* **193**, 5904–5913 (2014).
53. M. Levy, C. A. Thaiss, E. Elinav, Metabolites: Messengers between the microbiota and the immune system. *Genes Dev.* **30**, 1589–1597 (2016).
54. M. Veldhoen, C. Ferreira, Influence of nutrient-derived metabolites on lymphocyte immunity. *Nat. Med.* **21**, 709–718 (2015).
55. D. Michonneau, E. Latis, E. Curis, L. Dubouchet, S. Ramamoorthy, B. Ingram, R. P. de Latour, M. Robin, F. S. de Fontbrune, S. Chevret, L. Rogge, G. Socié, Metabolomics analysis of human acute graft-versus-host disease reveals changes in host and microbiota-derived metabolites. *Nat. Commun.* **10**, 5695 (2019).
56. C. G. Buffie, V. Bucci, R. R. Stein, P. T. McKenney, L. Ling, A. Gobourne, D. No, H. Liu, M. Kinnebrew, A. Viale, E. Littmann, M. R. M. van den Brink, R. R. Jenq, Y. Taur, C. Sander, J. R. Cross, N. C. Toussaint, J. B. Xavier, E. G. Pamer, Precision microbiome reconstitution restores bile acid mediated resistance to Clostridium difficile. *Nature* **517**, 205–208 (2015).
57. G. Roda, E. Porru, K. Katsanos, A. Skamnelos, K. Kyriakidi, G. Fiorino, D. Christodoulou, S. Danese, A. Roda, Serum bile acids profiling in inflammatory bowel disease patients treated with anti-TNFs. *Cell* **8**, 817 (2019).
58. A. M. Curtis, M. M. Bellet, P. Sassone-Corsi, L. A. J. O'Neill, Circadian clock proteins and immunity. *Immunity* **40**, 178–186 (2014).
59. K. Man, A. Loudon, A. Chawla, Immunity around the clock. *Science* **354**, 999–1003 (2016).
60. Y. Wu, B. Tao, T. Zhang, Y. Fan, R. Mao, Pan-cancer analysis reveals disrupted circadian clock associates with T cell exhaustion. *Front. Immunol.* **10**, 2451 (2019).
61. A. A. Lin, S. E. Wojciechowski, D. A. Hildeman, Androgens suppress antigen-specific T cell responses and IFN-γ production during intracranial LCMV infection. *J. Neuroimmunol.* **226**, 8–19 (2010).
62. A.-C. Lundell, I. Nordström, K. Andersson, A. Strömbeck, C. Ohlsson, Å. Tivesten, A. Rudin, Dihydrotestosterone levels at birth associate positively with higher proportions of circulating immature/naïve CD5 + B cells in boys. *Sci. Rep.* **7**, 15503 (2017).
63. M.-L. Zhu, P. Bakhru, B. Conley, J. S. Nelson, M. Free, A. Martin, J. Starmer, E. M. Wilson, M. A. Su, Sex bias in CNS autoimmune disease mediated by androgen control of autoimmune regulator. *Nat. Commun.* **7**, 11350 (2016).
64. A. C. Roden, M. T. Moser, S. D. Tri, M. Mercader, S. M. Kuntz, H. Dong, A. A. Hurwitz, D. J. McKean, E. Celis, B. C. Leibovich, J. P. Allison, E. D. Kwon, Augmentation of T cell levels and responses induced by androgen deprivation. *J. Immunol.* **173**, 6098–6108 (2004).
65. M. Walecki, F. Eisel, J. Klug, N. Baal, A. Paradowska-Dogan, E. Wahle, H. Hackstein, A. Meinhardt, M. Fijak, Androgen receptor modulates *Foxp3* expression in $CD4^+CD25^+Foxp3^+$ regulatory T-cells. *Mol. Biol. Cell* **26**, 2845–2857 (2015).
66. J. Linden, F. Koch-Nolte, G. Dahl, Purine release, metabolism, and signaling in the inflammatory response. *Annu. Rev. Immunol.* **37**, 325–347 (2019).
67. R. K. Iyer, H. K. Kim, R. W. Tsoa, W. W. Grody, S. D. Cederbaum, Cloning and characterization of human agmatinase. *Mol. Genet. Metab.* **75**, 209–218 (2002).
68. R. S. Hesterberg, J. L. Cleveland, P. K. Epling-Burnette, Role of polyamines in immune cell functions. *Med. Sci.* **6**, 22 (2018).
69. U. Bachrach, S. Persky, Interaction of oxidized polyamines with DNA: V. Inhibition of nucleic acid synthesis. *Biochim. Biophys. Acta* **179**, 484–493 (1969).
70. B. Francke, Cell-free synthesis of herpes simplex virus DNA: The influence of polyamines. *Biochemistry* **17**, 5494–5499 (1978).
71. K. Ito, K. Igarashi, Polyamine regulation of the synthesis of thymidine kinase in bovine lymphocytes. *Arch. Biochem. Biophys.* **278**, 277–283 (1990).
72. M. Zhang, T. Caragine, H. Wang, P. S. Cohen, G. Botchkina, K. Soda, M. Bianchi, P. Ulrich, A. Cerami, B. Sherry, K. J. Tracey, Spermine inhibits proinflammatory cytokine synthesis in human mononuclear cells: A counterregulatory mechanism that restrains the immune response. *J. Exp. Med.* **185**, 1759–1768 (1997).
73. V. Bronte, P. Zanovello, Regulation of immune responses by L-arginine metabolism. *Nat. Rev. Immunol.* **5**, 641–654 (2005).
74. R. Geiger, J. C. Rieckmann, T. Wolf, C. Basso, Y. Feng, T. Fuhrer, M. Kogadeeva, P. Picotti, F. Meissner, M. Mann, N. Zamboni, F. Sallusto, A. Lanzavecchia, L-Arginine modulates T cell metabolism and enhances survival and anti-tumor activity. *Cell* **167**, 829–842.e13 (2016).
75. J. R. Passweg, H. Baldomero, C. Chabannon, G. W. Basak, S. Corbacioglu, R. Duarte, H. Dolstra, A. C. Lankester, M. Mohty, S. Montoto, R. Peffault de Latour, J. A. Snowden, J. Styczynski, I. Yakoub-Agha, N. Kröger; European Society for Blood and Marrow

Transplantation (EBMT), The EBMT activity survey on hematopoietic-cell transplantation and cellular therapy 2018: CAR-T's come into focus. *Bone Marrow Transplant.* **55**, 1604–1613 (2020).
76. C. G. Rickert, J. F. Markmann, Current state of organ transplant tolerance. *Curr. Opin. Organ Transplant.* **24**, 441–450 (2019).
77. S. Li, N. L. Sullivan, N. Rouphael, T. Yu, S. Banton, M. S. Maddur, M. McCausland, C. Chiu, J. Canniff, S. Dubey, K. Liu, V. Tran, T. Hagan, S. Duraisingham, A. Wieland, A. K. Mehta, J. A. Whitaker, S. Subramaniam, D. P. Jones, A. Sette, K. Vora, A. Weinberg, M. J. Mulligan, H. I. Nakaya, M. Levin, R. Ahmed, B. Pulendran, Metabolic phenotypes of response to vaccination in humans. *Cell* **169**, 862–877.e17 (2017).
78. T. Lakshmikanth, A. Olin, Y. Chen, J. Mikes, E. Fredlund, M. Remberger, B. Omazic, P. Brodin, Mass cytometry and topological data analysis reveal immune parameters associated with complications after allogeneic stem cell transplantation. *Cell Rep.* **20**, 2238–2250 (2017).
79. F. G. Lakkis, R. I. Lechler, Origin and biology of the allogeneic response. *Cold Spring Harb. Perspect. Med.* **3**, a014993 (2013).
80. P. Khandelwal, A. Lane, V. Chaturvedi, E. Owsley, S. M. Davies, D. Marmer, A. H. Filipovich, M. B. Jordan, R. A. Marsh, Peripheral blood CD38 bright $CD8^+$ effector memory T cells predict acute graft-versus-host disease. *Biol. Blood Marrow Transplant.* **21**, 1215–1222 (2015).
81. P. Khandelwal, V. Chaturvedi, E. Owsley, A. Lane, D. Heyenbruch, C. M. Lutzko, T. Leemhuis, M. S. Grimley, A. S. Nelson, S. M. Davies, M. B. Jordan, R. A. Marsh, $CD38^{bright}CD8^+$ T cells associated with the development of acute GVHD are activated, proliferating, and cytotoxic trafficking cells. *Biol. Blood Marrow Transplant.* **26**, 1–6 (2020).
82. A. Stikvoort, Y. Chen, E. Rådestad, J. Törlén, T. Lakshmikanth, A. Björklund, J. Mikes, A. Achour, J. Gertow, B. Sundberg, M. Remberger, M. Sundin, J. Mattsson, P. Brodin, M. Uhlin, Combining flow and mass cytometry in the search for biomarkers in chronic graft-versus-host disease. *Front. Immunol.* **8**, 717 (2017).
83. K. A. Hogan, C. C. S. Chini, E. N. Chini, The multi-faceted ecto-enzyme CD38: Roles in immunomodulation, cancer, aging, and metabolic diseases. *Front. Immunol.* **10**, 1187 (2019).
84. S. Chatterjee, A. Daenthanasanmak, P. Chakraborty, M. W. Wyatt, P. Dhar, S. P. Selvam, J. Fu, J. Zhang, H. Nguyen, I. Kang, K. Toth, M. Al-Homrani, M. Husain, G. Beeson, L. Ball, K. Helke, S. Husain, E. Garrett-Mayer, G. Hardiman, M. Mehrotra, M. I. Nishimura, C. C. Beeson, M. G. Bupp, J. Wu, B. Ogretmen, C. M. Paulos, J. Rathmell, X.-Z. Yu, S. Mehrotra, CD38-NAD^+axis regulates immunotherapeutic anti-tumor T cell response. *Cell Metab.* **27**, 85–100.e8 (2018).
85. A. J. Covarrubias, R. Perrone, A. Grozio, E. Verdin, NAD^+ metabolism and its roles in cellular processes during ageing. *Nat. Rev. Mol. Cell Biol.* **22**, 119–141 (2021).
86. K. Wilhelm, J. Ganesan, T. Müller, C. Dürr, M. Grimm, A. Beilhack, C. D. Krempl, S. Sorichter, U. V. Gerlach, E. Jüttner, A. Zerweck, F. Gärtner, P. Pellegatti, F. Di Virgilio, D. Ferrari, N. Kambham, P. Fisch, J. Finke, M. Idzko, R. Zeiser, Graft-versus-host disease is enhanced by extracellular ATP activating P2X7R. *Nat. Med.* **16**, 1434–1438 (2010).
87. S. Pagliuca, D. Michonneau, F. Sicre de Fontbrune, A. Sutra Del Galy, A. Xhaard, M. Robin, R. Peffault de Latour, G. Socie, Allogeneic reactivity-mediated endothelial cell complications after HSCT: A plea for consensual definitions. *Blood Adv.* **3**, 2424–2435 (2019).
88. N. J. Gloude, P. Khandelwal, N. Luebbering, D. T. Lounder, S. Jodele, M. N. Alder, A. Lane, A. Wilkey, K. E. Lake, B. Litts, S. M. Davies, Circulating dsDNA, endothelial injury, and complement activation in thrombotic microangiopathy and GVHD. *Blood* **130**, 1259–1266 (2017).
89. S. A. Wall, Q. Zhao, M. Yearsley, L. Blower, A. Agyeman, P. Ranganathan, S. Yang, H. Wu, M. Bostic, S. Jaglowski, J. E. Brammer, B. William, H. Choe, A. S. Mims, S. Penza, Y. Efebera, S. Devine, S. Cataland, S. M. Davies, S. Vasu, Complement-mediated thrombotic microangiopathy as a link between endothelial damage and steroid-refractory GVHD. *Blood Adv.* **2**, 2619–2628 (2018).
90. Q. Ma, D. Li, R. Nurieva, R. Patenia, R. Bassett, W. Cao, A. M. Alekseev, H. He, J. J. Molldrem, M. H. Kroll, R. E. Champlin, G. E. Sale, V. Afshar-Kharghan, Reduced graft-versus-host disease in C3-deficient mice is associated with decreased donor Th1/Th17 differentiation. *Biol. Blood Marrow Transplant.* **18**, 1174–1181 (2012).
91. Q. Ma, D. Li, R. Carreño, R. Patenia, K. Y. Tsai, M. Xydes-Smith, A. M. Alousi, R. E. Champlin, G. E. Sale, V. Afshar-Kharghan, Complement component C3 mediates Th1/Th17 polarization in human T-cell activation and cutaneous GVHD. *Bone Marrow Transplant.* **49**, 972–976 (2014).
92. J. Camacho-Pereira, M. G. Tarragó, C. C. S. Chini, V. Nin, C. Escande, G. M. Warner, A. S. Puranik, R. A. Schoon, J. M. Reid, A. Galina, E. N. Chini, CD38 dictates age-related NAD decline and mitochondrial dysfunction through an SIRT3-dependent mechanism. *Cell Metab.* **23**, 1127–1139 (2016).
93. Y. Björk, E. Smith Knutsson, C. Ankarberg-Lindgren, A.-K. Broman, I. Andersson, L. Björkman, J. Magnusson, K. Bergmark, H. Anderson, P.-O. Andersson, M. Brune, Androgens in women after allogeneic hematopoietic cell transplantation: Impact of chronic GvHD and glucocorticoid therapy. *Bone Marrow Transplant.* **52**, 431–437 (2017).
94. T. W. Buford, D. S. Willoughby, Impact of DHEA(S) and cortisol on immune function in aging: A brief review. *Appl. Physiol. Nutr. Metab.* **33**, 429–433 (2008).
95. E. Velardi, J. J. Tsai, A. M. Holland, T. Wertheimer, V. W. C. Yu, J. L. Zakrzewski, A. Z. Tuckett, N. V. Singer, M. L. West, O. M. Smith, L. F. Young, F. M. Kreines, E. R. Levy, R. L. Boyd, D. T. Scadden, J. A. Dudakov, M. R. M. van den Brink, Sex steroid blockade enhances thymopoiesis by modulating Notch signaling. *J. Exp. Med.* **211**, 2341–2349 (2014).
96. N. J. Olsen, P. Zhou, H. Ong, W. J. Kovacs, Testosterone induces expression of transforming growth factor-beta1 in the murine thymus. *J. Steroid Biochem. Mol. Biol.* **45**, 327–332 (1993).
97. E. Clave, I. L. Araujo, C. Alanio, E. Patin, J. Bergstedt, A. Urrutia, S. Lopez-Lastra, Y. Li, B. Charbit, C. R. MacPherson, M. Hasan, B. L. Melo-Lima, C. Douay, N. Saut, M. Germain, D.-A. Trégouët, P.-E. Morange, M. Fontes, D. Duffy, J. P. Di Santo, L. Quintana-Murci, M. L. Albert, A. Toubert; Milieu Intérieur Consortium, Human thymopoiesis is influenced by a common genetic variant within the *TCRA-TCRD* locus. *Sci. Transl. Med.* **10**, eaao2966 (2018).
98. M. R. Gubbels Bupp, T. N. Jorgensen, Androgen-induced immunosuppression. *Front. Immunol.* **9**, 794 (2018).
99. M. V. Sitkovsky, T regulatory cells: Hypoxia-adenosinergic suppression and re-direction of the immune response. *Trends Immunol.* **30**, 102–108 (2009).
100. E. Hayase, D. Hashimoto, K. Nakamura, C. Noizat, R. Ogasawara, S. Takahashi, H. Ohigashi, Y. Yokoi, R. Sugimoto, S. Matsuoka, T. Ara, E. Yokoyama, T. Yamakawa, K. Ebata, T. Kondo, R. Hiramine, T. Aizawa, Y. Ogura, T. Hayashi, H. Mori, K. Kurokawa, K. Tomizuka, T. Ayabe, T. Teshima, R-Spondin1 expands Paneth cells and prevents dysbiosis induced by graft-versus-host disease. *J. Exp. Med.* **214**, 3507–3518 (2017).
101. S. Takashima, M. Kadowaki, K. Aoyama, M. Koyama, T. Oshima, K. Tomizuka, K. Akashi, T. Teshima, The Wnt agonist R-spondin1 regulates systemic graft-versus-host disease by protecting intestinal stem cells. *J. Exp. Med.* **208**, 285–294 (2011).
102. Y. Inamoto, P. J. Martin, S. J. Lee, A. A. Momin, L. Tabellini, L. E. Onstad, J. Pidala, M. E. D. Flowers, R. L. Lawler, H. Katayama, S. Hanash, J. A. Hansen, Dickkopf-related protein 3 is a novel biomarker for chronic GVHD after allogeneic hematopoietic cell transplantation. *Blood Adv.* **4**, 2409–2417 (2020).
103. S. Hubert, B. Rissiek, K. Klages, J. Huehn, T. Sparwasser, F. Haag, F. Koch-Nolte, O. Boyer, M. Seman, S. Adriouch, Extracellular NAD^+ shapes the $Foxp3^+$ regulatory T cell compartment through the ART2-P2X7 pathway. *J. Exp. Med.* **207**, 2561–2568 (2010).
104. M. Ashburner, C. A. Ball, J. A. Blake, D. Botstein, H. Butler, J. M. Cherry, A. P. Davis, K. Dolinski, S. S. Dwight, J. T. Eppig, M. A. Harris, D. P. Hill, L. Issel-Tarver, A. Kasarskis, S. Lewis, J. C. Matese, J. E. Richardson, M. Ringwald, G. M. Rubin, G. Sherlock, Gene Ontology: Tool for the unification of biology. *Nat. Genet.* **25**, 25–29 (2000).
105. The Gene Ontology Consortium, The Gene Ontology resource: 20 years and still GOing strong. *Nucleic Acids Res.* **47**, D330–D338 (2019).
106. K. Sidiropoulos, G. Viteri, C. Sevilla, S. Jupe, M. Webber, M. Orlic-Milacic, B. Jassal, B. May, V. Shamovsky, C. Duenas, K. Rothfels, L. Matthews, H. Song, L. Stein, R. Haw, P. D'Eustachio, P. Ping, H. Hermjakob, A. Fabregat, Reactome enhanced pathway visualization. *Bioinformatics* **33**, 3461–3467 (2017).
107. J. Spidlen, K. Breuer, C. Rosenberg, N. Kotecha, R. R. Brinkman, FlowRepository: A resource of annotated flow cytometry datasets associated with peer-reviewed publications. *Cytometry A* **81A**, 727–731 (2012).
108. K. Haug, K. Cochrane, V. C. Nainala, M. Williams, J. Chang, K. V. Jayaseelan, C. O'Donovan, MetaboLights: A resource evolving in response to the needs of its scientific community. *Nucleic Acids Res.* **48**, D440–D444 (2020).
109. T. Barrett, S. E. Wilhite, P. Ledoux, C. Evangelista, I. F. Kim, M. Tomashevsky, K. A. Marshall, K. H. Phillippy, P. M. Sherman, M. Holko, A. Yefanov, H. Lee, N. Zhang, C. L. Robertson, N. Serova, S. Davis, A. Soboleva, NCBI GEO: Archive for functional genomics data sets—Update. *Nucleic Acids Res.* **41**, D991–D995 (2013).
110. H. M. Schoemans, S. J. Lee, J. L. Ferrara, D. Wolff, J. E. Levine, K. R. Schultz, B. E. Shaw, M. E. Flowers, T. Ruutu, H. Greinix, E. Holler, G. Basak, R. F. Duarte, S. Z. Pavletic; EBMT (European Society for Blood and Marrow Transplantation) Transplant Complications Working Party and the "EBMT–NIH (National Institutes of Health)–CIBMTR (Center for International Blood and Marrow Transplant Research) GvHD Task Force, EBMT-NIH-CIBMTR Task Force position statement on standardized terminology & guidance for graft-versus-host disease assessment. *Bone Marrow Transplant.* **53**, 1401–1415 (2018).
111. A. H. Filipovich, D. Weisdorf, S. Pavletic, G. Socie, J. R. Wingard, S. J. Lee, P. Martin, J. Chien, D. Przepiorka, D. Couriel, E. W. Cowen, P. Dinndorf, A. Farrell, R. Hartzman, J. Henslee-Downey, D. Jacobsohn, G. McDonald, B. Mittleman, J. D. Rizzo, M. Robinson, M. Schubert, K. Schultz, H. Shulman, M. Turner, G. Vogelsang, M. E. D. Flowers, National Institutes of Health consensus development project on criteria for clinical trials in chronic graft-versus-host disease: I. Diagnosis and staging working group report. *Biol. Blood Marrow Transplant.* **11**, 945–956 (2005).

112. L. Ford, A. D. Kennedy, K. D. Goodman, K. L. Pappan, A. M. Evans, L. A. D. Miller, J. E. Wulff, B. R. Wiggs, J. J. Lennon, S. Elsea, D. R. Toal, Precision of a clinical metabolomics profiling platform for use in the identification of inborn errors of metabolism. *J. Appl. Lab. Med.* **5**, 342–356 (2020).
113. A. Dobin, T. R. Gingeras, Mapping RNA-seq reads with STAR. *Curr. Protoc. Bioinformatics* **51**, 11.14.1–11.14.19 (2015).
114. C. D. Dehaven, A. M. Evans, H. Dai, K. A. Lawton, Organization of GC/MS and LC/MS metabolomics data into chemical libraries. *J. Chem.* **2**, 9 (2010).
115. C. D. DeHaven, A. M. Evans, H. Dai, K. A. Lawton, Software techniques for enabling high-throughput analysis of metabolomic datasets.*Metabolomics* 10.5772/31277 (2012).

Acknowledgments: We thank all members of the CRYOSTEM Consortium and of the Francophone Society of Marrow Transplantations and Cellular Therapy (SFGM-TC) for providing patients samples used in this study and for support: University Hospital of Angers, University Hospital of Dijon Bourgogne, University Hospital of Besançon, University Hospital of Grenoble, University Hospital of Lille, University Hospital of Lyon, University Hospital of Bordeaux, Paoli-Calmettes Institute, AP-HM, University Hospital of Nantes, AP-HP (Saint-Louis Hospital, La Pitié-Salpêtrière hospital, Saint-Antoine Hospital, Robert Debré Hospital, Necker Hospital, Groupe Hospitalier Henri Mondor), INSERM, University Hospital of Toulouse, University Hospital of Tours, University Hospital of Rennes, University Hospital of Clermont-Ferrand, University Hospital of Saint-Etienne, Lucien Neuwirth Cancer Institute, University Hospital of Poitiers, University Hospital of Nice, University Hospital of Brest, Military Hospital of Percy, University Hospital of Montpellier, Gustave Roussy Institute, University Hospital of Limoges, University Hospital of Caen, and the Etablissement Français du Sang. We thank the technology platform team from the Institut de Recherche Saint Louis, Université de Paris for the quality control of our RNA samples. **Funding:** This project was funded by a grant from the Direction Générale de l'Offre de Soins (DGOS) and the Agence National de la Recherche (ANR) within a Projet de Recherche Translationnelle en Santé (ANR-PRTS 13002 to G.S.), by a research grant from Alexion Pharmaceutical company (APALEX to R.P.d.L. and G.S.), by the Institut National du Cancer (project number INCa 2014-1-PL BIO-07-IP-1 to G.S.), by a research grant from L'Association Laurette Fugain (ALF 2017/03 to D.M.), and by a research grant from Swiss Cancer Research Fundation (BIL KFS-3988-08-2016 to L.D.). CRYOSTEM project is supported by a grant from the Institut National du Cancer (INCa to R.P.d.L.) and the Agence Nationale de la Recherche (ANR to R.P.d.L.) and under the auspices of the Société Francophone de Greffe de Moelle et de Thérapie Cellulaire (SFGM-TC). **Author contributions:** Conceptualization: G.S. and D.M. Methodology: G.S. and D.M. Formal analysis: L.D. and N.V. A.C. and C.B. generated the mass cytometry data. L.D. gated the cells of interest using the Cytobank. H.T. preprocessed the mass cytometry, metabolomics, and transcriptomics data, with input from S.V.G., L.D., R.S. and D.M. R.S. did a statistical analysis of the clinical data. H.T. identified cell subpopulations in the mass cytometry data using FlowSOM, advised by S.V.G. L.D. manually annotated these subpopulations. A.B. performed RNA sequencing experiments with L.D. L.D., D.M., and B.I. performed metabolomics experiments. H.T. generated permutation distributions to identify features of interest in the three data sources, advised by R.S. H.T. identified correlations between features from the three data sources. L.D. and D.M. did enrichment analyses on the correlated metobolites and genes. H.T. integrated the mass cytometry, metabolomics, and transcriptomics data. D.M. and H.T. generated the figures. Investigation: L.D., A.C., C.B., H.Z., J.-F.D., B.I., and D.M. Resource: R.P.d.L.., D.M., and Y.S. Data curation: L.D. and D.M. Writing–original draft: L.D., H.T., G.S., and D.M. Writing–review and editing: Y.S., G.S., and D.M. Visualization: D.M. Supervision: G.S. and D.M. Project administration: G.S. and D.M. Funding acquisition: G.S., R.P.d.L., and D.M. **Competing interests:** G.S. and R.P.d.L. received a research grant from Alexion Pharmaceutical Company. R.P.d.L. received a research grant from Novartis and Pfizer companies. G.S. received fees from Pharmacyclics LLC, Novartis, Incyte, Alexion, Amgen, and Pfizer. D.M. received fees from Novartis, Incyte, Jazz Pharmaceuticals, and CSL Behring companies. All other authors declare that they have no competing interests. **Data and materials availability:** All data associated with this study present in the paper or the Supplementary Materials. Mass cytometry raw data are accessible on FlowRepository (*107*) under the accession number FR-FCM-Z2JP. Metabolomics raw data are available on MetaboLights repository (*108*) under the references MTBLS220 (cohort 1) and MTBLS221 (cohort 2). The RNA sequencing data discussed in this publication have been deposited in NCBI's Gene Expression Omnibus (GEO) (*109*) and are accessible through GEO series accession number GSE150735. The R code used for analysis is available at Zenodo (DOI: 10.5281/zenodo.5807544).

Submitted 23 December 2020
Resubmitted 26 October 2021
Accepted 28 December 2021
Published 23 February 2022
10.1126/scitranslmed.abg3083

Science Translational Medicine

Operational tolerance after hematopoietic stem cell transplantation is characterized by distinct transcriptional, phenotypic, and metabolic signatures

Laetitia DubouchetHelena TodorovRuth SeurinckNicolas ValletSofie Van GassenAurélien CorneauCatherine BlancHabib ZoualiAnne BolandJean-François DeleuzeBrian IngramRegis Peffault de LatourYvan SaeysGérard SociéDavid Michonneau

Sci. Transl. Med., 14 (633), eabg3083. • DOI: 10.1126/scitranslmed.abg3083

Understanding operational tolerance

Operational tolerance describes a spontaneous lack of alloreactivity to donor cells or tissue in the absence of immunosuppressive drugs. Although operational tolerance has been observed in solid organ transplantation and hematopoietic stem cell transplantation (HSCT), the features underlying operational tolerance are not clear. Here, Dubouchet *et al.* characterized the transcriptional, immunological, and metabolomic features of operational tolerance in two cohorts of individuals who received HSCT from an HLA-matched sibling donor. The authors found that operational tolerance was distinguished by expression of immunosuppressive markers, including CD73, as well as androgens. Together, these findings shed light on potential drivers of operational tolerance.